

A decrease in river discharge and rainfall amount, from a 100-year data set, in response to El Niño events on the interannual temporal scale for the Philippines

Natasha Sekhon¹, CP David², Mart Cyrel M. Geronia³, Manuel Justin G. Custado⁴, and Daniel Enrique Ibarra¹

¹Brown University

²University of the Philippines Diliman

³National Institute of Geological Sciences

⁴National Institute of Geological Sciences, University of the Philippines, Diliman

November 23, 2022

Abstract

The El Niño Southern Oscillation (ENSO) modulates rainfall amount variability and, by extension, river discharge in the Philippines on seasonal to interannual temporal scales. The El Niño phase (ENP) of ENSO considerably decreases rainfall amounts on a seasonal scale in the western Pacific with varying degrees of heterogeneity expressed across the Philippines. Our understanding of the response in the hydroclimate to ENPs on interannual timescales is still relatively immature. As such, to investigate the hydroclimate response, a composite time series of 29 rainfall and 61 river discharge stations spanning 1901-2020 and 1908-2017 C.E., respectively, and covering the four major climate types in the Philippines were assessed. Our results suggest, regardless of climate type, that river discharge and rainfall data decrease following ENPs. The median response suggests that the decreasing trend can last up to seven years. Further, the hydroclimate response follows either a decreasing trend, if at conception of an ENP, or an increasing trend, if at the termination of an ENP. As water-scarcity becomes an area of immediate concern in an increasingly warming climate, our results have implications for interannual water resource management in this drought-prone tropical archipelago.

1 **A decrease in river discharge and rainfall amount, from**
2 **a 100-year data set, in response to El Niño events on**
3 **the interannual temporal scale for the Philippines**

4 **Natasha Sekhon^{1,2}, Carlos Primo C. David³, Mart Cyrel M. Geronia³, Manuel**
5 **Justin G. Custado³, Daniel E. Ibarra^{1,2}**

6 ¹Department of Earth, Environmental and Planetary Science, Brown University, Providence, Rhode
7 Island 02912, USA

8 ²Institute at Brown for Environment and Society, Brown University, Providence, Rhode Island 02912,
9 USA

10 ³National Institute of Geological Sciences, University of the Philippines, Diliman, Quezon City, 1101,
11 Philippines

12 **Key Points:**

- 13 • A river discharge and rainfall data set spanning 100 years in the Philippines used
14 to analyze the hydroclimate response to El Niño periods.
- 15 • Composite river discharge and rainfall means, with seasonality and long-term trends
16 removed, show decrease following El Niño event where an event is sea surface tem-
17 perature $>1^{\circ}\text{C}$ in Nino 3.4 region.
- 18 • The decreasing trend in the hydroclimate variables can up to last several years us-
19 ing a Superposed Epoch Analysis.

Corresponding author: Natasha Sekhon, natasha_sekhon@brown.edu

Abstract

The El Niño Southern Oscillation (ENSO) modulates rainfall amount variability and, by extension, river discharge in the Philippines on seasonal to interannual temporal scales. The El Niño period (ENP) of ENSO considerably decreases rainfall amounts on a seasonal scale in the western Pacific with varying degrees of heterogeneity expressed across the Philippines. Our understanding of the response in the hydroclimate to ENPs on interannual timescales is still relatively immature. As such, to investigate the hydroclimate response, a composite time series of 29 rainfall and 61 river discharge stations spanning 1901-2020 and 1908-2017 C.E., respectively, and covering the four major climate types in the Philippines were assessed. Our results suggest, regardless of climate type, that river discharge and rainfall data decrease following ENPs. The median response suggests that the decreasing trend can last up to seven years. Further, the hydroclimate response follows either a decreasing trend, if at conception of an ENP, or an increasing trend, if at the termination of an ENP. As water-scarcity becomes an area of immediate concern in an increasingly warming climate, our results have implications for interannual water resource management in this drought-prone tropical archipelago.

1 Introduction

Coupled air-sea interactions of the El Niño Southern Oscillation (ENSO) in the Pacific Ocean lead to tropical drought conditions in the Philippines during El Niño (warm) phases on a seasonal temporal scale (Lyon, 2004; Lyon et al., 2006). The drought conditions during an El Niño phase of ENSO is induced by the late onset of the rainy season, early termination of the rainy season, or a weak monsoon system characterized by isolated heavy rainfall events of short-durations (Lansigan et al., 2000). Geographically, the Philippines is located in the western Pacific between 4°40'N to 21°10'N, 116°40'E to 126°34'E with over 7,000 islands in the archipelago (Figure 1a). The large agronomic sector of the Philippines relies on seasonal rainfall for crop production and multiple previous studies have highlighted the loss in crop production during El Niño events (Lansigan et al., 2000; Cinco et al., 2014; Stuecker et al., 2018). The seasonal response in rainfall as a result of El Niño events is spatially heterogeneous across the Philippines and continues to be an active area of research (Lyon, 2004; Lyon et al., 2006; Villafuerte II et al., 2014; Villafuerte et al., 2015). However, the legacy effects of El Niño events on the hydroclimate in the Philippines are still poorly understood and understudied in the literature. Further, the legacy effect of El Niño with respect to drought conditions (Kolusu et al., 2019), terrestrial ecosystems (Jorge-Romero et al., 2021), and coral reefs (Claar et al., 2018) highlight the need to investigate the response of hydroclimate to El Niño periods on an interannual temporal scale.

Understanding the relationship between the hydroclimate and El Niño periods on an interannual temporal scale is important for water resource management, especially since extreme El Niño events are predicted to increase in intensity and frequency due to anthropogenic-induced greenhouse warming (Cai et al., 2014). In this study we leverage 100-year long river discharge (1908-2017 C.E.) and rainfall amount (1901-2020 C.E.) data spatially spread across the Philippine archipelago to discern the relationship between hydroclimate variables and El Niño events for the 20th and 21st century. In this study, rainfall discharge data and rainfall amount data constitute the two hydroclimate variables of interest. Paired rainfall amount and river discharge response to ENSO phases provide a nuanced response to hydroclimate variability, which might be missed if only one of the two hydroclimate variables is used (Schmidt et al., 2001; Poveda et al., 2001; Poveda et al., 2011). River discharge acts an integration of rainfall over a given river basin and provides insight into the lagged response of the land-atmosphere water cycle. Rainfall data on the other hand is a closer reflection of the ocean-atmosphere water cycle and larger-scale dynamical moisture delivery (or lack thereof) due to ENSO teleconnections (Lyon et al., 2006). Next, to assess the range of hydroclimate responses to the El Niño

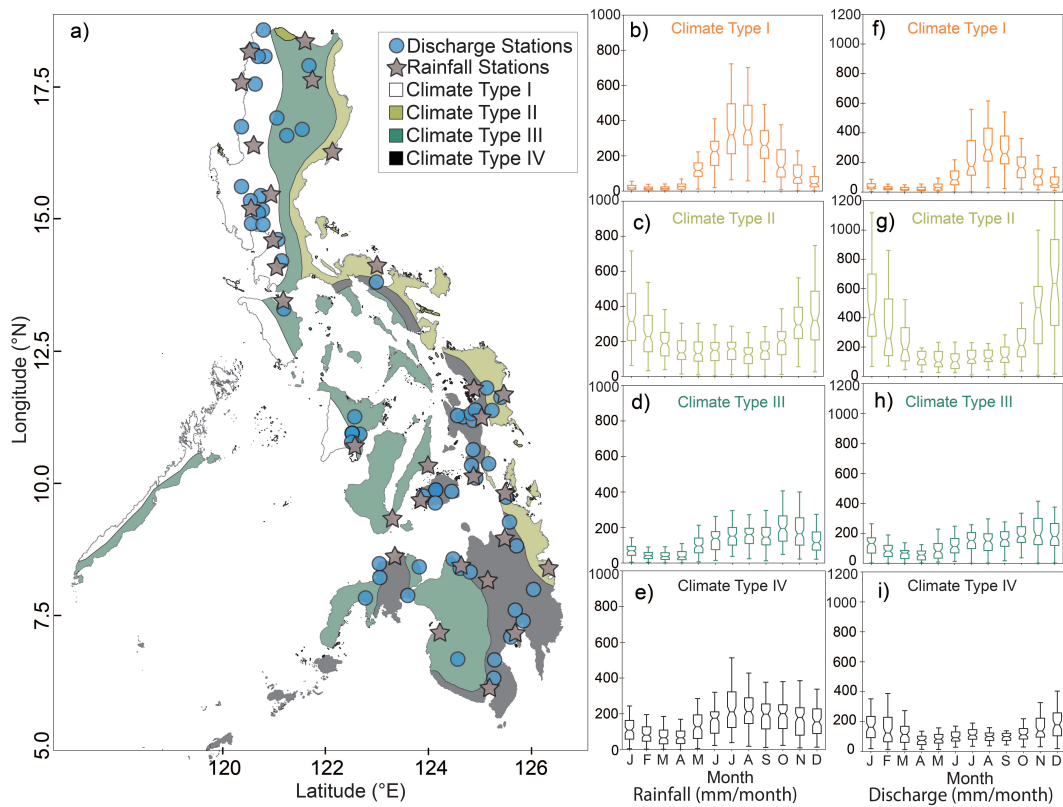


Figure 1. (a) Map of the Philippines with river discharge stations and rainfall amount stations used in this study. The prevalent climate types following Ibarra et al. (2021) (see also Makanas (1990); Jose and Cruz (1999); Tolentino et al. (2016)) are overlain with different colors. Rainfall and river discharge distribution for (b,f) Climate Type I, (c,g) Climate Type II, (d,h) Climate Type III, (e,i) Climate Type IV as monthly box plots highlight differences in the seasonality of the hydroclimate.

72 phase of ENSO, we conducted multiple sensitivity analyses using different criterion. First,
 73 we investigated the response to different intensities of El Niño events. Next, we inves-
 74 tigated the response at the beginning and termination of El Niño periods. An event typ-
 75 ifies a single time unit and a period typifies a duration of time. Lastly, to isolate the in-
 76 terannual temporal variability of the hydroclimate variables, we removed the seasonal
 77 and long-term trends from the composite time series. The composite time series were
 78 the mean river discharge and rainfall station data for the four different Climate Types.

79 In this work, Superposed Epoch Analysis suggests that rainfall and river discharge
 80 decrease at statistically significant values in response to the El Niño phase of ENSO. The
 81 duration of the decreasing trend can last up to seven years following the event of inter-
 82 est. Our sensitivity analyses highlight the nuanced hydroclimate response to the El Niño
 83 period. At the conception of an El Niño period, the hydroclimate variables decrease. Con-
 84 versely, at the termination of an El Niño period, hydroclimate variables increase towards
 85 wetter conditions. Further, rainfall has a quicker, albeit a smaller amplitude, response
 86 to the El Niño phase compared to river discharge. Our results have implications for wa-
 87 ter resource management avenues that traditionally investigate the seasonal response to
 88 the El Niño or La Niña phases of ENSO. As irrigation-dependent ecosystems address the
 89 growing scarcity of water (Perez-Blanco & Sapino, 2022), we highlight the legacy effects
 90 of El Niño and its implications for water resource management on an interannual tem-
 91 poral scale. Addressing tropical droughts modulated through El Niño and subsequent
 92 health concerns on an interannual temporal scale provides a framework to investigating
 93 long-term impacts of El Niño in the Philippines and global tropics (Kovats, 2000).

94 2 Methods and Data set Description

95 Four major climate types prevail in the Philippines based on the modified Coro-
 96 nas Classification, following Tolentino et al. (2016) and Ibarra et al. (2021) (Figure 1a;
 97 (Makanas, 1990; Jose & Cruz, 1999). River discharge (interchangeably termed here as
 98 streamflow) and rainfall data were subdivided following the four major climate types.
 99 Composite rainfall (averaged over 1901-2020 CE) and river discharge (averaged over 1908-
 100 2017 CE) climatologies reveal a distinct boreal summer wet season (June-October) for
 101 Climate Type I (Figure 1b and 1f) and a distinct boreal winter wet season (November-
 102 March) for Climate Type II (Figure 1c and 1g). Climate Type III (Figure 1d and 1h)
 103 and Climate Type IV (Figure 1e and 1i) have a less distinctive wet season.

104 River discharge and rainfall data, termed here as hydroclimate variables, were largely
 105 collated from multiple observation stations and one gridded spatial data set. The dif-
 106 ferent data sets are briefly described below. Data handling steps to construct compos-
 107 ite river discharge and rainfall time-series covering the 20th and 21st century for each cli-
 108 mate type are also described. All steps described herein were conducted using Python3.2
 109 (Van Rossum & Drake, 2009) and available as part of this publication (See Section 6).

110 2.1 River Discharge Data set

111 Monthly streamflow observations from 61 river discharge stations spanning 1908-
 112 2017 C.E. were analyzed in this study (Supplemental Table 1). Streamflow observation
 113 data for 55 stations from 1946 C.E. onwards come from Ibarra et al. (2021) and com-
 114 prise three Philippine data sets: Bureau of Research Standards data set, Global Runoff
 115 Data Centre data set, and Global Streamflow Indices and Metadata archive reference
 116 data set. The acquisition and processing of streamflow data for the 55 stations are dis-
 117 cussed in detail in Tolentino et al. (2016) and Ibarra et al. (2021). Briefly, the Philip-
 118 pines' Department of Public Works and Highways maintains records of river discharge
 119 data initially through the Bureau of Research and Standards and now through the Bu-
 120 reau of Design. The Global Runoff Data Center is a global data set that records river
 121 discharge data and was initiated with the World Meteorological Organization. Global

122 Streamflow Indices and Metadata archive is a collection of daily streamflow observations
123 (Gudmundsson et al., 2018).

124 We extend the Ibarra et al. (2021) streamflow observation data by incorporating
125 historical river discharge data that spanned 1908-1922 C.E for eight rivers. The histor-
126 ical river discharge data is the result of daily streamflow measurements between 1908-
127 1914 and 1918-1922 C.E. made by the Irrigation Division of the Bureau of Public Works
128 (Williams & Gochoco, 1924). Daily streamflow measurements were not made between
129 December 1914 and June 1918 due to lack of funds. Historical data for 53 rivers are avail-
130 able through the Bureau of Public Works. However, the daily measurements made were
131 sparse and sporadic (Williams & Gochoco, 1924). Therefore, the criteria for selecting
132 historical river discharge measurements in this study were twofold. First, data that ex-
133 tended the river discharge observations collated by Ibarra et al. (2021) were included.
134 Second, historical river discharge data that had measurements for nine or ten years (1908-
135 1913 and 1918-1922 C.E.) were included for further analyses. Eight historical river dis-
136 charge data met this criteria (BPW in Supplemental Table 1). In total, 61 river discharge
137 station data sets with monthly mean values of river discharge were included in this anal-
138 ysis (Supplemental Figure 1a-d). For this study, daily discharge measurements reported
139 in liters/second were averaged to monthly means and normalized by the drainage area
140 (units of sq. km), resulting in mm/month units, comparable to the data sets collated in
141 Ibarra et al. (2021). In cases where diurnal streamflow measurements were made, we first
142 took the daily average before down sampling to area normalized monthly means.

143 2.2 Rainfall Amount Data set

144 Monthly rainfall data from 29 stations spanning 1901-2020 C.E. were analyzed (Sup-
145 plemental Table 2, Supplemental Figure 2a-d). Data was collated from three different
146 data sets. The Philippine Weather Bureau (PWB) data set, later digitized and archived
147 by the Japan Agency for Marine-Earth Science and Technology (JAMSTEC), included
148 daily rainfall amounts spanning 1901-1940 C.E. for 65 stations across the Philippines (Kubota
149 et al., 2017). However, the measured rainfall amount data are sporadic and sparse, hence,
150 only PWB stations that had ten years of continuously measured rainfall data were se-
151 lected for analyses. 14 stations with daily rainfall data covering 1901-1940 C.E. met the
152 aforementioned criteria. The daily data were summed to give monthly rainfall totals in
153 mm/month. Next, the Asian Precipitation - Highly-Resolved Observational Data Inte-
154 gration Towards Evaluation (APHRODITE) contains a gridded daily rainfall amount in
155 inches based on a dense network of rain-gauge stations interpolated at $0.25 \times 0.25^\circ$ (Yatagai
156 et al., 2012). Rainfall data for 26 stations spanning 1951-1990 C.E. that extended either
157 the PWB station data or data from 1991-2020 C.E. (final data set) were incorporated
158 as monthly rainfall totals in mm/month. The final data set (denoted as modern in Sup-
159 plemental Table 2) is from the United States National Centers for Environmental Infor-
160 mation (NCEI), an official repository of climate data from the World Meteorological Or-
161 ganization (Makanas, 1990; Lawrimore et al., 2011). The Philippine Atmospheric, Geo-
162 physical, and Astronomical Services Administration (PAGASA) regularly deposits its
163 meteorological data in the NCEI. This third data set spans 1991-2020 C.E. Rainfall data
164 measured in inches was converted to monthly totals in mm. In order to include data with
165 extreme rainfall amounts and to make the rainfall data comparable to river discharge
166 data, daily rainfall data was summed to monthly rainfall totals. In this analysis, we are
167 interested in investigating the spatial and temporal hydroclimate response to the El Niño
168 phase of ENSO. In order to compare amplitude and lead and lag variability between rain-
169 fall and river discharge, we selected rainfall station data that was spatially and tempo-
170 rally equivalent to a river discharge station and within the same Climate Type (Figure
171 1a). Hence, we note that there are multiple additional rainfall station data from the PA-
172 GASA/NCEI data set that were not utilized in this study. Out of 58 NCEI stations, we
173 only used rainfall data from 28 stations spanning 1991-2020 C.E.

174

2.3 Developing Composite Time Series

175

176

177

178

Composite time-series based on Climate Types were constructed to maximize the length of measured river discharge and rainfall data for subsequent analysis. Data handling steps to construct river discharge and rainfall data composite time series are described:

179

180

181

182

183

184

185

186

187

188

189

190

191

192

193

194

195

196

197

198

199

200

1. Individual river discharge and rainfall data in monthly means (mm/month) and monthly sums (mm/month), respectively, were categorized according to the four major Climate Types.
2. The mean of the subset river discharge and rainfall data based on Climate Types were calculated. For example, the composite river discharge time series of Climate Type I is the mean of 17 river discharge stations. Similarly, the composite rainfall data time series of Climate Type I is the mean of seven rainfall amount stations.
3. The mean data were then log transformed to approximately conform to a normal distribution. The units are in log(mm/month).
4. The log transformed data were standardized, thereby data is unitless, by removing the mean and scaling to unit variance. Hence, variation on the y-axis of the composite time series is the departure from the log transformed mean.
5. A polynomial fit (order = 3), which best captured the shape of the long-term trend, was applied to the standardized data from Step 4. The long-term trend was removed to isolate the intrinsic variability in El Niño and to minimize anthropogenic induced variability. The resulting trend was then subtracted from the standardized data.
6. Finally, sub-seasonal and seasonal frequencies were removed from the detrended data to isolate the interannual variability of El Niño Cyclicality. The sub-seasonal and seasonal signal was removed by taking the 6 (± 3)- and 12 (± 6)- month centered moving average of each time series.

201

202

203

The resultant composite river discharge and rainfall time series based on the four different Climate Types were compared against the Nino3.4 Relative Index time series (next section).

204

2.4 Nino3.4 Relative Index

205

206

207

208

209

210

211

212

213

214

215

216

217

Multiple indices measuring Sea Surface Temperature (SST) anomalies in the tropical Pacific exist to track oscillations between El Niño, Neutral, and La Niña periods. Nino3.4 Index acts as a bellwether to forecast the onset of ENSO conditions (D. Chen et al., 2004). Nino3.4 is the average SST anomaly (departures from 1971-2000 C.E.) in the region bounded by 5°N to 5°S, from 170°W to 120°W. Local SST changes in this region, which is indicative of changing deep tropical convection and atmospheric circulation, are critical for affecting rainfall variability over the Philippines (Lyon, 2004). Recent studies highlight the importance in removing the SST tropical trends to increase the sensitivity of the indices in relation to climate change (Turkington et al., 2019; Van Oldenborgh et al., 2021). The Nino3.4 Relative Index is the Nino3.4 SST anomaly after removing the tropical (20°S-20°N) ocean SST trend (Van Oldenborgh et al., 2021). The SST values used in this study are from the Extended Reconstructed Sea Surface Temperatures Version 5 and span 1854-2020 C.E. (Huang et al., 2017).

218

219

220

221

222

223

An El Niño period changes in its SST definition depending on the cited study. For example, Trenberth (1997) defines an El Niño period if SST anomalies (SSTA) in the Nino3.4 region exceed 0.4°C for 6 months or more. In contrast, NCEI characterizes an El Niño period by time-periods when SSTA in the Nino3.4 region exceeds 0.5°C for 5 months (Dole et al., 2018). Lastly, the National Climate Center classifies an El Niño period if SSTA in the Nino3.4 region exceeds 0.8°C, which is approximately 1 standard deviation

greater than the average SST (Nicholls, 1991). Given the range in definitions of what constitutes an El Niño period, in this analysis we considered an El Niño period when SSTA in the Nino3.4 region exceeded 1°C for 3 months or more. Next, normal El Niño events are classified as deviations of 1°C or greater. Lastly, extreme El Niño events are classified by a deviation of 2.2°C or greater in the Nino3.4 region, following the 1997/97 and 2015/16 events (Santoso et al., 2017). To assess the response of the background (noise) tropical Pacific conditions, a superfluous signal with a minimally positive SSTA is defined when SSTA in the Nino3.4 region range between 0 to 0.2°C .

2.5 Hydroclimate Response to El Niño Events

Multiple Superposed Epoch Analysis (SEA) with different criteria were conducted to evaluate the range in response of the hydroclimate variables (river discharge and rainfall) to El Niño events and periods. SEA is a statistical test that identifies the link, magnitude, and significance between discrete events and continuous time series within a probabilistic framework, which is optimized by averaging across all events (Haurwitz & Brier, 1981). Recently, a modified double-bootstrap SEA framework (Rao et al., 2019) that quantifies uncertainty in the median response and in the natural background variability has been used to investigate ENSO (Dee et al., 2020), drought (Gazol & Tíscar, 2020), and river discharge (Rao et al., 2020). Briefly, the median response in a SEA is a deviation in climatology from a pre-event time frame covering a post-event time frame. A total window length of 11 years, which covers 3 years pre-event to 7 years post-event was used in our study. Year 0, therefore corresponds to an El Niño event in the format of YYYY-MM. Detailed methodology for the double-bootstrap SEA is described in Rao et al. (2019). SEA was not conducted on historical (1901-1940 C.E.) river discharge data due to a lack of sufficient and continuous data but was nevertheless included in our time series for graphical comparison with contemporaneous rainfall data. To capture the whole range in the hydroclimate response, SEA was conducted on the composite river discharge and rainfall data with five different categories/criterion of what defines an event of interest.

1. Category I/Normal El Niños: A discrete time-series list where every month with SSTA in Nino3.4 Relative Index is greater than 1°C and is thus considered an El Niño event of interest.
2. Category II/Extreme El Niños: A discrete time-series list with only extreme El Niños, defined when SSTA in Nino3.4 Relative Index is greater than 2.2°C . If multiple consecutive months have SSTA's greater than 2.2°C , only the month with the largest SSTA was considered an event of interest. Therefore, the discrete time-series is constructed with the peak of extreme El Niños.
3. Category III/Conception of an El Niño period: A discrete time-series that defines an event of interest as the first month during an El Niño period of at least 3 continuous months greater than 1°C .
4. Category IV/Termination of an El Niño period: A discrete time-series that defines an event of interest as the last month during an El Niño period of at least 3 continuous months greater than 1°C .
5. Category V/Superfluous Signal Response: A discrete time-series that defines an event of interest within the neutral phase where SSTA is between 0 and 0.2°C .

The categories therefore capture different flavors during ENSO's El Niño phase. Category I and II capture the intensities of El Niño events. Category III and IV together capture the response of the hydroclimate variables during the life-cycle (i.e., conception to termination) of an El Niño period. Category V (superfluous signal) was added to assess the validity of the SEA between signal and background conditions of the tropical Pacific. The 5th percentile, median, and 95th percentile hydroclimate response is calculated from 1,000 composite matrices using unique subsets of N events at random without replacement from the discrete event time-series. N events randomly selected repre-

275 sent approximately half the total number of events for each category. Events that were
 276 beyond the post-year time period were not included. For example, 2015-05, is an El Niño
 277 event of interest under Category I, however, the post-event 7-year period dates to 2022-
 278 05 C.E. As there is no hydroclimate or SST data (yet) available for that period, 2015-
 279 05 is not included in the discrete time-series, which signifies the events of interest. The
 280 1st, 5th, 10th, 90th, 95th, 99th significance thresholds needed to be exceeded for the SEA
 281 response to be significant were calculated using random bootstrap generated by draw-
 282 ing pseudo events over the entire time series for the same number of (N) events (Brad Adams
 283 et al., 2003). The significance thresholds provide a robust assessment such that when the
 284 response crosses the threshold there is high confidence that the response is not a ran-
 285 dom signal. The superfluous signal category falls within neutral conditions of ENSO atmosphere-
 286 ocean dynamics. The category assesses whether it is the El Niño phase of ENSO that
 287 contributes to the hydroclimate response or neutral tropical Pacific Ocean conditions.
 288 If the hydroclimate response to Category V is the same for Category I-IV as shown by
 289 SEA, delineating between El Niño or neutral conditions as the causal mode modulat-
 290 ing the hydroclimate response would be difficult.

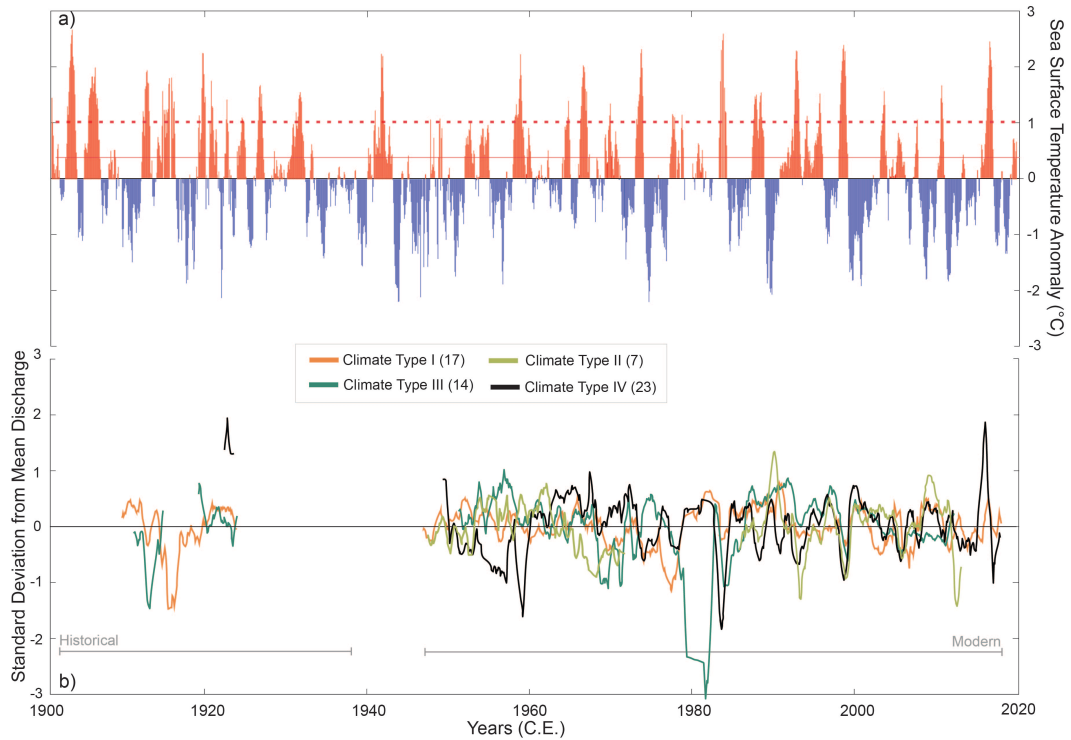


Figure 2. (a) Sea-surface temperature anomalies (SSTA) for the Nino3.4 region with the tropical trend removed (Nino3.4 rel. index). (b) Time-series of river discharge data based on different climate types region for the 20th and 21st century. The red dashed line indicates extreme El Niño events. The red solid line indicates criteria for superfluous signal sensitivity test. N is the number of river discharge stations in each Climate Type to calculate a composite record.

291 3 Results

292 The composite river discharge and rainfall time series with the long-term trend and
 293 seasonal signal removed for the four climate types compared against Nino3.4 Relative
 294 Index are shown in Figure 2 and 3, respectively. The composite hydroclimate time se-
 295 ries covers historical (1901-1940 C.E.) and modern (1950 - 2020 C.E.) periods. The re-
 296 sults from the data handling steps to obtain the composite time series for the four Cli-
 297 mate Types for river discharge and rainfall data are in Supplemental Figure 3-6 and Fig-
 298 ure 8-11, respectively. The polynomial fit to remove the long-term trend and the sub-
 299 sequent detrended river discharge and rainfall data are in Supplemental Figure 7a-h and
 300 Figure 12a-h.

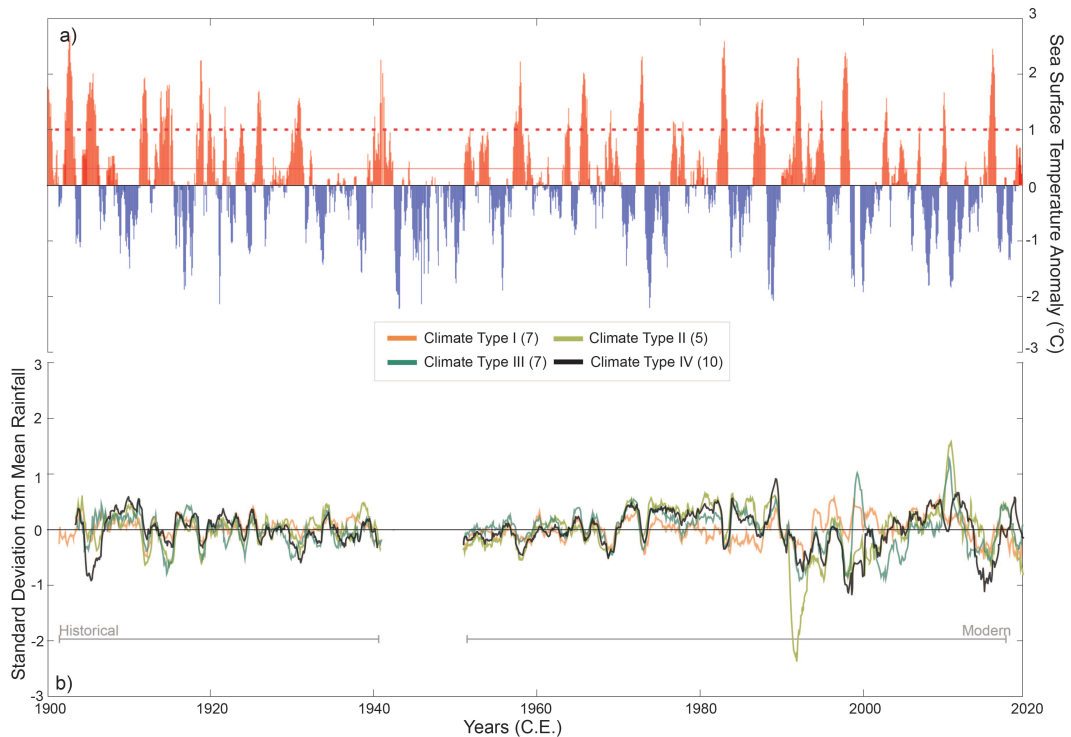


Figure 3. (a) Sea-surface temperature anomalies (SSTA) for the Nino3.4 region with the tropical trend removed (Nino3.4 rel. index). (b) Time-series of rainfall data based on different climate types region for the 20th and 21st century. The red dashed line indicates extreme El Niño events. The red solid line indicates criteria for superfluous signal sensitivity test. N is the number of rainfall stations in each Climate Type to calculate a composite record.

301 3.1 Seasonal Distribution of El Niño events

302 The highest number of El Niño events in Category I/Normal El Niños (see Section
 303 2.5. for definitions of different Categories) occur during the boreal winter (October-February)
 304 months (Figure 4a and 4e). For all four Climate Types, El Niño events of interest in Cat-
 305 egory I of composite river discharge and rainfall data occur throughout the year. April
 306 is the month with the lowest number of El Niño events. The extreme El Niño event (Cat-
 307 egory II), which is typically the peak (a single month) with SSTA's greater than 2.2°C

falls during the boreal winter months (Figure 4b and 4f). This is in agreement with literature suggesting that boreal winter is the maturation period for the Niño3.4 region in the Pacific Ocean (McPhaden, 2003). Here we define the conception of an El Niño period as the first month of at least three continuous months with SSTA's greater than 1°C (Category III) filtered from events in Category I. The seasonal distribution of Category III events is bimodal over Spring (April-June) and Winter (October-January) months (Figure 4c and 4g). The termination of the El Niño period is the last month of at least a three-month period with SSTA's greater than 1°C (Category IV) filtered from events in Category I. A majority of events in Category IV occur during the boreal late winter/early spring (February - March) months (Figure 4d and 4h); hence, suggesting that the conception of El Niño events occur in spring or winter. Conversely, El Niño periods terminate in the winter. Seemingly, El Niño events of interest are absent (for Category II, III, IV) during the boreal summer months of July-September. This highlights the complex nature of investigating El Niño response to hydroclimate variability on the seasonal scale. The variation in the number of counts in river discharge and rainfall data (y-axis in Figure 4) lies in the time-continuous nature of the composite time-series for the four major Climate Type. A strength of Superposed Epoch Analysis is that it provides a response to an aggregated event list. Further, the removal of the seasonal signal and long-term trends from the composite river discharge and rainfall amount data provides an opportunity to investigate responses on intra to interannual scales.

3.2 River Discharge Response to Different El Niño Criterion

River discharge for all Climate Types shows strong and statistically significant decreases in the years following El Niño events of interest and lasting up to three to five years where an event is defined as any time (YYYY-MM) with SSTA greater than 1°C (Table 1a and Figure 5a). The decreasing trend and the magnitude varies based on the Climate Type. The strongest decrease in discharge (median response), relative to the three-year pre-event mean, occurs three years post-event (i.e. year 0 + 3 on the x-axis) before increasing (at a statistical significance) to pre-event mean for Climate Type I (orange crosses in Figure 5a). The 5th and 95th percentile response (orange shading in Figure 5a) represents the degree of uncertainty based on 1000 unique sets of 50 El Niño events from a total of 103 potential events. Similarly, for Climate Type II (where the SSTA threshold is 2.2°C, extreme El Niños), the strongest decrease in discharge (median response) occurs five years post-event (Table 1a) before increasing (olive green crosses in Figure 5a). The magnitude (amplitude) of river discharge decrease is the most severe and the trend lasts the longest for Climate Type II compared to the remaining three Climate Types. The magnitude and length of decrease in river discharge for Climate Type III is similar to Climate I's response: strongest decrease in discharge (median response) occurs four years post-event (dark green crosses in Figure 5a). However, the increase in discharge is more staggered in Climate Type III compared to Climate Type I. The decrease and increase in river discharge (median response) for Climate Type IV (black crosses in Figure 5a) follows a similar pattern to Climate Type III. However, the amplitude of decrease is approximately two times more severe in Climate Type IV than Climate Type I for Category I.

In Category II (Table 1b), river discharge for all Climate Types shows a strong decrease in the years following extreme El Niño events and lasting up to four (Climate Type I) or seven (Climate Type II and IV) years. The decrease in river discharge, relative to the pre-event mean, is statistically not significant for Climate Type III. The magnitude of the strongest decrease is for rivers in Climate Type II (-0.7 on the y-axis). The decrease in river discharge for Climate Types I is followed by an increase to pre-event mean climatology.

Our SEA results for Category III that take a subset at the conception of a El Niño periods (Table 1c) suggest a decrease in river discharge (median response) for all Climate

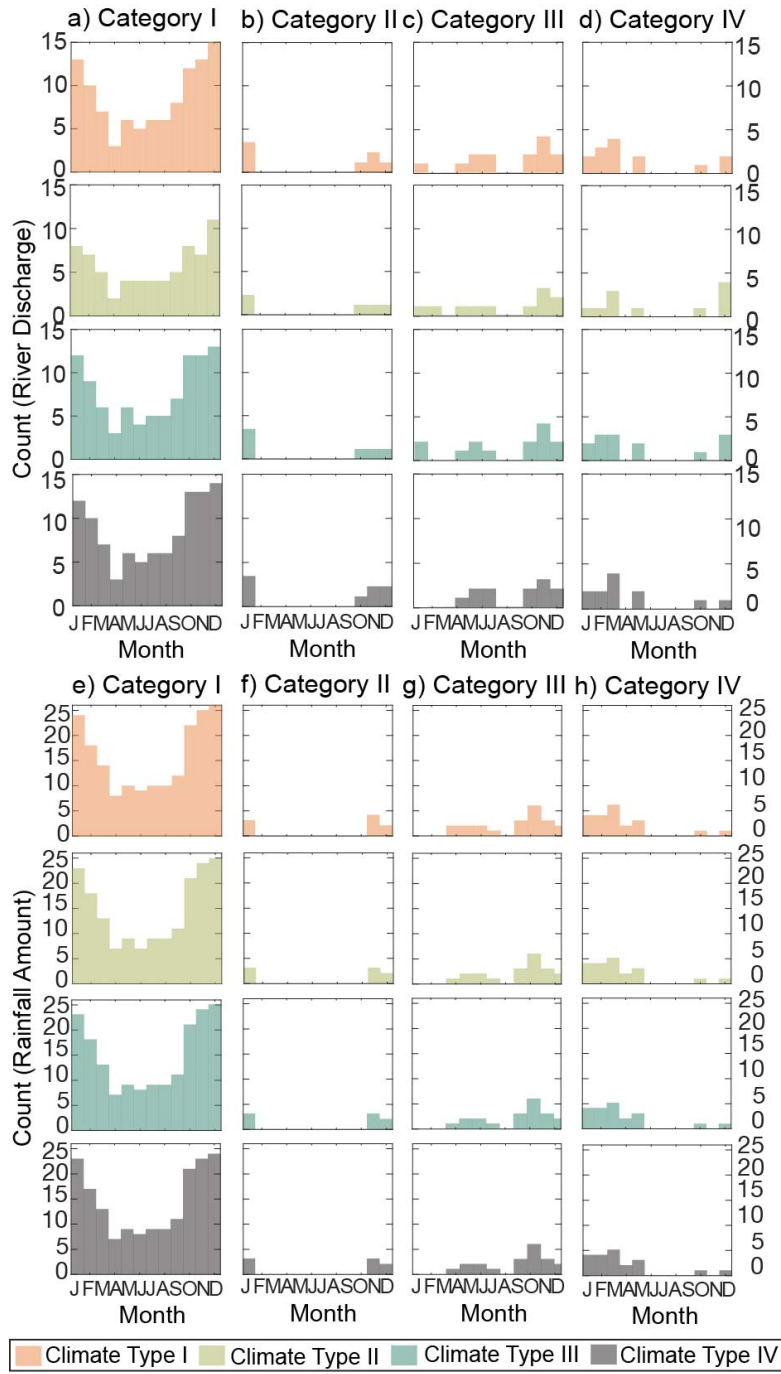


Figure 4. Histogram demonstrating the monthly timing of El Niño events for Superposed Epoch Analysis sensitivity tests that fall under Category I (a,e), Category II (b,f), Category III (c,g), Category IV (d,h) for the four different Climate Types. Columns a) to d) show the monthly distribution of El Niño events for river discharge (modern) composite time series. Columns e) to h) depict the distribution of El Niño events for rainfall (historical + modern) time series.

Table 1. Sensitivity tests investigating the response of discharge to different categories of El Niño events using Superposed Epoch Analysis

Sensitivity Criteria	Number of Events	Post-Event Response	Max. Response Year (Amplitude)	Statistical Significance	
a) Category I/ Normal El Niños: SSTA > 1°C					
Climate Type I	103	↓ 1-3 yr ; ↑ 4-7yr	+ 3 (-0.10)	1%	Intensity Category El Niño
Climate Type II	67	↓ 1-5 yr ; ↑ 6-7yr	+ 5 (-0.20)	1%	
Climate Type III	94	↓ 1-4 yr ; ↑ 5-7yr	+ 4 (-0.10)	5%	
Climate Type IV	103	↓ 1-4 yr ; ↑ 5-7yr	+ 4 (-0.20)	1%	
b) Category II/ Extreme El Niños: SSTA > 2.2 °C					
Climate Type I	6	↓ 1-4 yr ; ↑ 5-7yr	+ 4 (-0.15)	5%	Intensity Category El Niño
Climate Type II	5	↓ 1-7 yr	+ 7 (-0.70)	1%	
Climate Type III	6	↓ 1- 2yr ; ↑ 2-7yr	+ 1 (-0.10)	<i>Not Significant</i>	
Climate Type IV	8	↓ 1-7 yr	+ 3 (-0.40)	1%	
c) Category III/ Conception of an El Niño Period: First month in an El Niño Period where SSTA > 1°C					
Climate Type I	12	↓ 1-7 yr	+ 7 (-0.30)	1%	Timing within El Niño Period Category
Climate Type II	11	↓ 1-7 yr	+ 7 (-0.20)	<i>Not Significant</i>	
Climate Type III	11	↓ 1-5 yr ; ↑ 6-7yr	+ 5 (-0.20)	10%	
Climate Type IV	12	↓ 1-7 yr	+ 7 (-0.50)	1%	
d) Category IV/ Termination of an El Niño Period: Last month in an El Niño Period where SSTA > 1°C					
Climate Type I	12	↑ 1-7yr	+ 7 (0.30)	95%	Timing within El Niño Period Category
Climate Type II	11	↓ 1-5 yr ; ↑ 6-7yr	+ 5 (-0.50)	<i>Not Significant</i>	
Climate Type III	11	↑ 1-7yr	+ 7 (0.25)	90%	
Climate Type IV	12	↑ 1-7yr	+ 7 (0.40)	90%	
e) Category V/Superflous Signal Check: 0.2°C < SSTA > 0°C					
Climate Type I	70	↑ 1-7yr	+ 7 (0.05)	95%	Noise Category
Climate Type II	41	↓ 1-3 yr ; ↑ 4-7yr	+ 3 (0.05)	95%	
Climate Type III	56	↓ 1-7 yr	+ 7 (0.05)	<i>Not Significant</i>	
Climate Type IV	68	↑ 1-7yr	+ 7 (0.05)	<i>Not Significant</i>	

Types. The decreasing trend lasts between five (Climate Type III) and seven (Climate Type I and IV) years. The magnitude of the strongest decrease is for rivers in Climate Type IV (-0.5 on the y-axis). The median response is statistically not significant for Climate Type II. Conversely, our SEA results for Category IV that takes a subset at the termination of an El Niño period (Table 1d) suggests an increase in river discharge (median response) for Climate Types I, III, and IV. The increasing river discharge trend lasts for seven years for the three Climate Types. The magnitude of the strongest increase, similar to Category III, is for rivers in Climate Type IV (0.4 on the y-axis). River discharge decreases at a statistically insignificant level for Climate Type II.

To ascertain the response of neutral conditions or the background variability (Category V), our SEA result suggests an increase for Climate Type I and II. The response in Climate Type III and IV is statistically insignificant. The superfluous signal response is the opposite from Category I and II, which are the normal and extreme El Niño events. Further the amplitude of the response is much smaller (0.05) compared to the response when using different El Niño criterion. Therefore, this analysis adds confidence that the response in river discharge to El Niño events in the Nino3.4 region is a robust deviation from the neutral climate conditions.

Table 2. Sensitivity tests investigating the response of historical rainfall data to different categories of El Niño events using Superposed Epoch Analysis

Sensitivity Criteria	Number of Events	Post-Event Response	Max. Response Year (Amplitude)	Statistical Significance	
a) Category I/ Normal El Niños: SSTA > 1°C					
Climate Type I	83	↓ 1-4 yr ; ↑ 5-7yr	+ 4 (-0.02)	1%	Intensity Category El Niño
Climate Type II	71	↓ 1-2 yr ; ↑ 3-7yr	+ 2 (-0.10)	1%	
Climate Type III	72	↓ 1-2 yr ; ↑ 3-7yr	+ 2 (-0.10)	1%	
Climate Type IV	69	↓ 1-2 yr ; ↑ 3-7yr	+ 2 (-0.10)	1%	
b) Category II/ Extreme El Niños: SSTA > 2.2 °C					
Climate Type I	3	Not Enough			Intensity Category El Niño
Climate Type II	2	Events			
Climate Type III	2	For SEA			
Climate Type IV	2				
c) Category III/ Conception of an El Niño Period: First month in an El Niño Period where SSTA > 1°C					
Climate Type I	9	↓ 1-7 yr	+ 7 (-0.20)	1%	Timing within El Niño Period Category
Climate Type II	8	↓ 1-7 yr	+ 7 (-0.20)	1%	
Climate Type III	8	↓ 1-7 yr	+ 7 (-0.30)	10%	
Climate Type IV	8	↓ 1-7 yr	+ 7 (-0.30)	5%	
d) Category IV/ Termination of an El Niño Period: Last month in an El Niño Period where SSTA > 1°C					
Climate Type I	9	↑ 1-7yr	+ 7 (0.20)	95%	Timing within El Niño Period Category
Climate Type II	8	↑ 1-7yr	+ 7 (0.30)	95%	
Climate Type III	8	↑ 1-7yr	+ 7 (0.30)	95%	
Climate Type IV	8	↑ 1-7yr	+ 7 (0.30)	99%	
e) Category V/Superfluous Signal Check: 0.2°C < SSTA > 0°C					
Climate Type I	56	↑ 1-7yr	+ 7 (0.05)	95%	Noise Category
Climate Type II	55	↑ 1-5 yr ; ↓ 6-7yr	+ 5 (0.10)	95%	
Climate Type III	55	↑ 1-2 yr ; ↓ 3-7yr	+ 2 (0.05)	95%	
Climate Type IV	68	↑ 1-2 yr ; ↓ 3-7yr	+ 2 (0.05)	95%	

3.3 Rainfall Amount Response to Different El Niño Criterion

Historical (Table 2a) and modern (Table 3a) rainfall response for all Climate Types shows strong and significant decrease in the years following El Niño events and lasting up to two to four years where an event is defined as any time period with SSTA greater than 1°C (Figure 5b and 5c). That said, the magnitude of decrease is not as strong as the response observed in river discharge. Second, the recovery to pre-event mean climatology is faster by two to three years in both historical and modern rainfall response compared to the river discharge response for Category I, likely demonstrating importance of aquifer storage and transient storage even in tropical settings with (relatively) small catchments such as in the Philippines.

The low number of events in Category II for the historical rainfall data (Table 2b) precludes a formal SEA assessment. However, SEA shows a decreasing trend in the modern rainfall at a statistical significance level for Climate III and IV in response to extreme El Niño events (Category II). This is similar to the river discharge response to years following extreme El Niño events. The median response in rainfall suggests an increase to pre-event mean conditions after three years following the strongest decrease in rainfall amount. Rainfall response is not significant for Climate Type I and is not included in the subsequent discussion. The increase in Climate Type II is statistically significant at the 90th confidence level (Table 3b) for modern rainfall data. This response in the hydroclimate stands out as an outlier compared to the modern rainfall response in Climate Types III and IV.

4 Discussion

4.1 Hydroclimate Response to the Intensity of El Niño Events

Following normal (Category I) and extreme (Category II) El Niño events, rainfall and river discharge decrease relative to the pre-event three-year hydroclimate means. The duration of the decreasing trend lasts between three to seven years from the event year (0 on the x-axis) depending on the Climate Type and intensity of the El Niño event (Table 1a-b, 2a-b, 3a-c). Next, the decreasing trend in river discharge lags by one or two years compared to the rainfall. Alternatively, rainfall recovers to the pre-event hydroclimate mean faster by one or two years compared to river discharge. Lastly, we found that the amplitude of response is greater for river discharge compared to rainfall (Figure 6). The difference in the amplitude and the duration of the decreasing trend is likely attributed to multiple factors that govern river discharge and streamflow conditions. Variability in streamflow conditions are sensitive to effective rainfall amount, vegetation type, size and slope of catchment area, bedrock lithology, baseflow conditions, and floodplain/aquifer storage (Stoelzle et al., 2014; Yang et al., 2017). Comparatively, rainfall amount is intimately linked to ocean-atmosphere dynamics in the western Pacific Ocean (Lyon, 2004). Further, the composite time series used in the SEA to assess the response is following the removal of seasonal and long-term trends. Therefore, the varied response in amplitude/magnitude and duration within the different Climate Types for Category I (normal El Niño events) suggests that land-surface features such as vegetation and soil type, as well as dependency on agricultural intake, antecedent soil moisture conditions, and balance between precipitation and evapotranspiration might be important factors modulating the amplitude and the duration of the response. Finally, consistent trends in the duration and amplitude of rainfall response for historical (Table 2a) and modern (Table 3a) time between Climate Types suggest that the El Niño phase of the ENSO dynamics over the 20th and 21st century modulate rainfall consistently through the observed time.

The large magnitude and consistent decrease in the hydroclimate using the peak of extreme El Niño (Category II) events suggests the legacy of El Niño events could lead

Table 3. Sensitivity tests investigating the response of modern rainfall data to different categories of El Niño events using Superposed Epoch Analysis

Sensitivity Criteria	Number of Events	Post-Event Response	Max. Response Year (Amplitude)	Statistical Significance	
a) Category I/ Normal El Niños: SSTA > 1°C					
Climate Type I	105	↓ 1-4 yr ; ↑ 5-7yr	+ 4 (-0.02)	1%	Intensity Category El Niño
Climate Type II	105	↓ 1-2 yr ; ↑ 3-7yr	+ 2 (-0.02)	1%	
Climate Type III	105	↓ 1-3 yr ; ↑ 4-7yr	+ 3 (-0.10)	1%	
Climate Type IV	103	↓ 1-4 yr ; ↑ 5-7yr	+ 4 (-0.10)	1%	
b) Category II/ Extreme El Niños: SSTA > 2.2 °C					
Climate Type I	6	↓ 1-7 yr	+ 7 (-0.02)	Not Significant	Timing within El Niño Period Category
Climate Type II	6	↑ 1-7yr	+ 7 (0.30)	90%	
Climate Type III	6	↓ 1-3 yr ; ↑ 4-7yr	+ 3 (-0.10)	5%	
Climate Type IV	6	↓ 1-3 yr ; ↑ 4-7yr	+ 3 (-0.10)	5%	
c) Category III/ Conception of an El Niño Period: First month in an El Niño Period where SSTA > 1°C					
Climate Type I	12	↓ 1-7 yr	+ 7 (-0.15)	1%	Noise Category
Climate Type II	12	↓ 1-4 yr ; ↑ 5-7yr	+ 4 (-0.20)	1%	
Climate Type III	12	↓ 1-5 yr ; ↑ 6-7yr	+ 5 (-0.15)	10%	
Climate Type IV	12	↓ 1-7 yr	+ 7 (-0.40)	1%	
d) Category IV/ Termination of an El Niño Period: Last month in an El Niño Period where SSTA > 1°C					
Climate Type I	12	↑ 1-7yr	+ 7 (0.05)	Not Significant	
Climate Type II	12	↑ 1-7yr	+ 7 (0.40)	95%	
Climate Type III	12	↑ 1-7yr	+ 7 (0.30)	99%	
Climate Type IV	12	↑ 1-7yr	+ 7 (0.30)	95%	
e) Category V/Superfluous Signal Check: 0.2°C < SSTA > 0°C					
Climate Type I	77	↓ 1-7 yr	+ 7 (-0.01)	Not Significant	
Climate Type II	77	↓ 1-7 yr	+ 7 (-0.01)	Not Significant	
Climate Type III	77	↓ 1-7 yr	+ 7 (-0.01)	Not Significant	
Climate Type IV	77	↓ 1-7 yr	+ 7 (-0.01)	Not Significant	

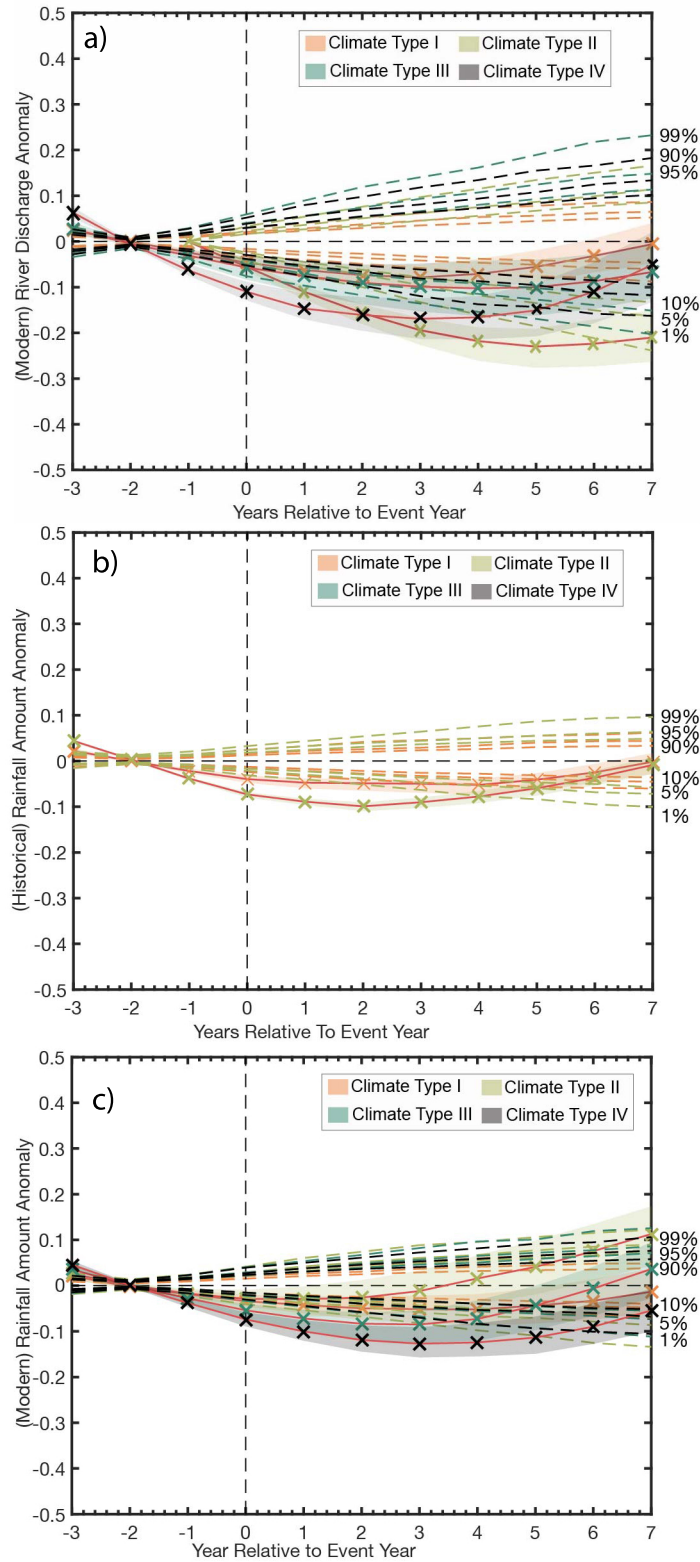


Figure 5. Superposed Epoch Analysis (SEA) showing (a) river discharge, (b) historical rainfall, and (c) modern rainfall response to El Niño events where an event is from a discrete time-series with months corresponding to SSTA's greater than 1°C. Uncertainty intervals for the different Climate Types are 5th and 95th percentiles of the hydroclimate response, while the sub-horizontal lines indicate the threshold required for the epochal median anomalies (red lines) to be statistically significant using random bootstrapping at three different confidence intervals. Climate Type III and IV response for the historical rainfall amount (b) is the same as Climate Type III and hence not clearly visible.

427 to potential long-term (multi-year) droughts. The peak of the extreme El Niño is con-
 428 sidered an event of interest in Category II. The subsequent ensuing event list comprises
 429 events in the 1950s (Event: 1957-12), 1960s (Event: 1966-01), 1970s, (Event: 1972-12)
 430 1980s (Event: 1982), and 1990s (1992-01). Each decade in our event list is attributed
 431 to prevalent drought conditions in Southeast Asia (Sheffield & Wood, 2007; Venkatappa
 432 et al., 2021). Further, long-term drought conditions in Southeast Asia are attributed to
 433 the El Niño phase of ENSO (Harger, 1995). However, not all severe El Niño events guar-
 434 antee the nascence of droughts (Harger, 1995). Our SEA results for the extreme El Niño
 435 events suggests that the decreasing trend in response to extreme El Niño (Table 1b and
 436 3b) potentially reflects El Niño induced long-term droughts. The decreasing hydrocli-
 437 mate trend continues for up to seven years relative to the pre-event hydroclimate mean
 438 for both river discharge and rainfall composite time series. Our results are in-line with
 439 investigations into river and rainfall response to ENSO on an interannual to interdecadal
 440 temporal scale in Australia (Simpson et al., 1993; Arblaster et al., 2002; Rimbu et al.,
 441 2004). The studies investigate the long-term or legacy effects of ENSO on rainfall (Arblaster
 442 et al., 2002) and streamflow (Rimbu et al., 2004) variability. Rimbu et al. (2004) found
 443 that streamflow variability is strongly correlated to the Niño3 index during the 1900s to
 444 1930s. Our study places the framework of hydroclimate variables responding to the in-
 445 tensity of El Niño events on a response temporal scale lasting on an interannual scale.
 446 The latter is an advancement as most studies investigate the seasonal response of ENSO
 447 (Schmidt et al., 2001). SEA further allows us to observe an aggregate response, which
 448 is useful when investigating El Niño events as characteristics of individual El Niño events
 449 are known to be slightly different (Harger, 1995; Wang et al., 2019).

450 **4.2 Temporal Placement in the El Niño Period Dictates the Trend in** 451 **the Hydroclimate Response**

452 ENSO is not the only source of forcing for tropical droughts but is known to mod-
 453 ulate droughts in the global tropics on the interannual and interdecadal temporal scale
 454 (Krishnamurthy & Goswami, 2000; Lyon, 2004, 2004; Mendoza et al., n.d.; L. Chen et
 455 al., 2021). Here, we discuss how the temporal placement in an El Niño period (Category
 456 III and IV) impacts the response in the hydroclimate variables in the Philippines. At
 457 the onset of an El Niño period, our results suggest that hydroclimate variables decrease
 458 up to seven years (Table 1c, 2c, 3c). Conversely, at the termination of an El Niño pe-
 459 riod (Category IV), hydroclimate variables increase as quickly as three years (Table 1d,
 460 2d, 3d). The difference in the response based on the temporal placement (i.e., season-
 461 ally or inter annually) in an El Niño period highlights the importance of variability be-
 462 tween conception and termination of El Niño periods. For example, 1957-04 is an event
 463 at the onset of a continuous El Niño period that lasted until 1958-04. Seven years post
 464 1957-04 is 1964-04 and during this interval ENSO oscillates between neutral, La Niña,
 465 and El Niño phases (Figure 2a and 3a). Conversely, the termination of the El Niño pe-
 466 riod (1958-04) is bracketed on the pre-event side with El Niño conditions (1955-04) and
 467 with a majority of La Niña and neutral phases of ENSO on the post-event side. Sim-
 468 ilarly, the 1997-05 event is the onset of a continuous El Niño period that lasted until 1998-
 469 03. The pre-event conditions largely fall in the El Niño phase of ENSO and the post-
 470 event conditions cover neutral, La Niña, and El Niño phases of ENSO. The difference
 471 in the hydroclimate variable response to the placement in an El Niño period implies sen-
 472 sitivity to antecedent surface conditions (Zhu et al., 2007). The conception of an El Niño
 473 period (Category III) is followed by El Niño, neutral and La Niña phases of ENSO. The
 474 reduction in the convective rainfall circulation system over southeast Asia during the con-
 475 ception of an El Niño period leads to a decrease in rainfall data, which lasts up to seven
 476 years and is clearly visible in the historical rainfall data (Table 2c). Further, the pre-event
 477 mean is likely during a La Niña or neutral phase, and the antecedent conditions are less
 478 likely to be drought prone. Hence, the deviation from the pre-event mean is large. Con-
 479 versely, the inverse is the case for the hydroclimate response at the termination of an El

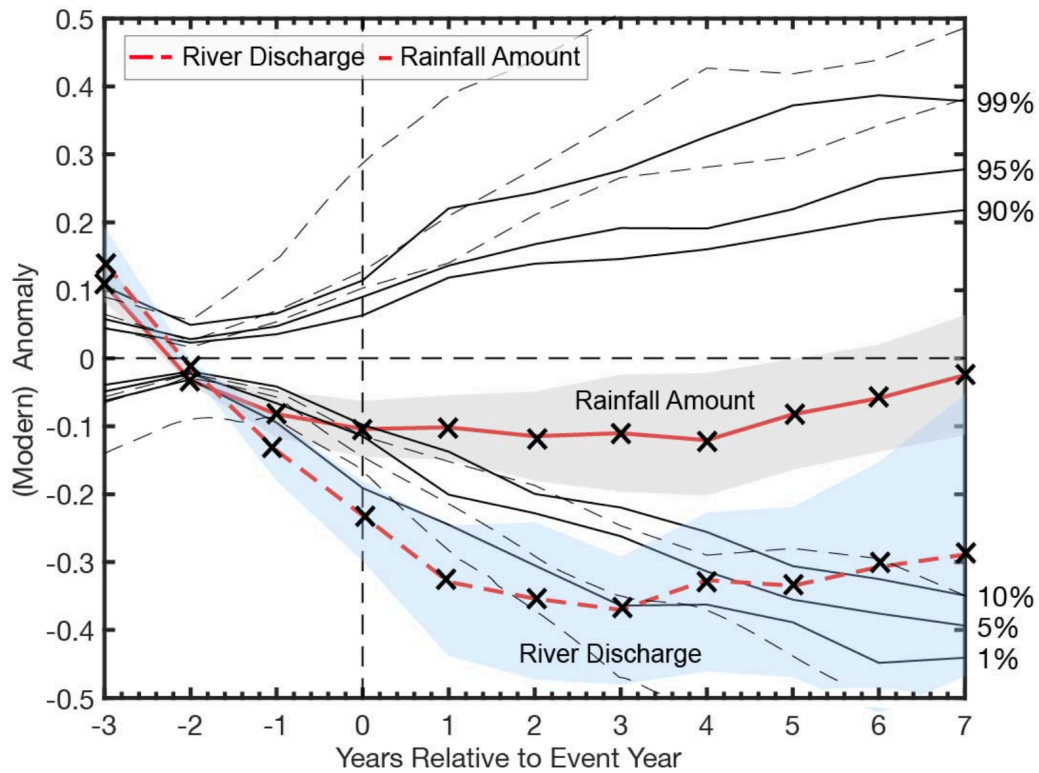


Figure 6. Superposed Epoch Analysis showing modern river discharge (dashed) and rainfall (solid) rainfall response to extreme El Niño events (Category IV) for Climate Type IV. Uncertainty intervals are 5th and 95th percentiles of the hydroclimate response, while the sub-horizontal lines indicate the threshold required for the epochal median anomalies (red lines) to be statistically significant using random bootstrapping at three different confidence intervals. River discharge has a larger amplitude in response to events. Conversely, rainfall has a smaller response and recovers faster to the pre-event mean.

480 Niño period. The antecedent conditions are more acutely reflective of drought conditions.
 481 Next, the post-event years are followed by neutral to La Niña conditions. Therefore, the
 482 general response in hydroclimate is to increase following the termination of El Niño pe-
 483 riods. The duration of the response is consistently up to seven years (Table 1d, 2d, 3d)
 484 regardless of river discharge or rainfall data. This highlights the relatively quick response
 485 to wet conditions (La Niña) compared to dry conditions (El Niño).

486 5 Conclusions

487 Philippines is a nation of over 7,000 islands and it heavily relies on rainfall to main-
 488 tain groundwater and streamflow resources. Understanding the interannual hydrolog-
 489 ical dynamics of island nations such as the Philippines is imperative to better plan for
 490 water resource management (Higley & Conroy, 2019). In our analysis, we utilized a 100-
 491 year paired river discharge and rainfall data to ascertain the hydroclimate response to
 492 varying intensities and duration of El Niño periods. The mean, log-normalized, scaled,
 493 detrended with the seasonal signal removed composite time series for the four major Cli-
 494 mate Types was compared against the Niño3.4 Relative Index to discern the interannual
 495 response using SEA analysis. Our analysis suggests that the hydroclimate variables de-
 496 crease in response to normal and extreme El Niño events. The duration of the decreas-
 497 ing trend lasts up to three (normal El Niño events) or seven (extreme El Niño events)
 498 years following the event. Further, the hydroclimate metrics respond differently based
 499 on the temporal placement (conception to termination) of the event during an El Niño
 500 period. Composite river discharge and rainfall data decrease up to seven years follow-
 501 ing the conception of an El Niño period. Conversely, the hydroclimate response is to in-
 502 crease up to seven years following the termination of an El Niño period. The magnitude
 503 of response is lagged in discharge compared to rainfall amount data sets. Further, rain-
 504 fall amount recovers faster to pre-event means following decreasing trends than river dis-
 505 charge data. The former is more intimately linked to direct ocean-atmosphere dynam-
 506 ics than river discharge data, which depends on multiple hydrological parameters. This
 507 is the first study to the best of our knowledge that attempts to quantify the sign, mag-
 508 nitude, and severity of the hydroclimate response to El Niño events for the Philippines
 509 on an interannual temporal scale using over 100 years of available data sets. Our results
 510 have implication for regions that are prone to tropical droughts and are agrarian soci-
 511 eties (Kovats, 2000; Wang et al., 2019; Perez-Blanco & Sapino, 2022). With further de-
 512 velopment of transfer functions between hydroclimate variables and El Niño indices the
 513 fidelity of end of 21st century simulations can be tested (Li et al., 2006; Perry et al., 2020).

514 6 Open Research

515 Code written in Python was used for all data reduction and statistical analyses.
 516 The code is stored in a GitHub repository: <https://doi.org/10.5281/zenodo.6079558> Data
 517 required for running the code can be found at in the repository: (will be made available
 518 via Zenodo during publication). Superposed Epoch Analysis was implemented follow-
 519 ing the Matlab code by (Rao et al., 2019).

520 Acknowledgments

521 The authors would like to thank Pamela Louise M. Tolentino for access to historic
 522 data sets, Sebastian Muñoz on feedback on the manuscript and Dr. Victor Tsai for dis-
 523 cussions. We thank Drs. Ryan Edgar and Karishma Sekhon of ExitPi LLC for useful con-
 524 versations and computational references. Dr. Natasha Sekhon was funded by the Voss
 525 Postdoctoral Research and Presidential Postdoc Fellowship awards from Brown Univer-
 526 sity. This research was initiated by a DOST-PCIEERD Balik Scientist award to Dr. Daniel
 527 E. Ibarra.

528 **References**

- 529 Arblaster, J., Meehl, G., & Moore, A. (2002). Interdecadal modulation of australian
530 rainfall. *Climate Dynamics*, *18*(6), 519–531.
- 531 Brad Adams, J., Mann, M. E., & Ammann, C. M. (2003). Proxy evidence for an el
532 nino-like response to volcanic forcing. *Nature*, *426*(6964), 274–278.
- 533 Cai, W., Borlace, S., L., W., & England, M. (2014). Increasing frequency of extreme
534 el niño events due to greenhouse warming. *Nature Climate Change*, *4*(2), 111–
535 116.
- 536 Chen, D., Cane, M. A., Kaplan, A., Zebiak, S. E., & Huang, D. (2004). Predictabil-
537 ity of el niño over the past 148 years. *Nature*, *428*(6984), 733–736.
- 538 Chen, L., Li, G., Long, S.-M., Gao, C., Zhang, Z., & Lu, B. (2021). Interdecadal
539 change in the influence of el niño in the developing stage on the central china
540 summer precipitation. *Climate Dynamics*, 1–18.
- 541 Cinco, T. A., de Guzman, R. G., & David M. Wilson, F. D. H. (2014). Long-
542 term trends and extremes in observed daily precipitation and near surface
543 air temperature in the philippines for the period 1951–2010. *Atmospheric*
544 *Research*, 12–26.
- 545 Claar, D. C., Szostek, L., McDevitt-Irwin, J. M., Schanze, J. J., & Baum, J. K.
546 (2018). Global patterns and impacts of el niño events on coral reefs: A meta-
547 analysis. *PLoS One*, *13*(2), e0190957.
- 548 Dee, S. G., Cobb, K. M., Emile-Geay, J., Ault, T. R., Edwards, R. L., Cheng, H., &
549 Charles, C. D. (2020). No consistent enso response to volcanic forcing over the
550 last millennium. *Science*, *367*(6485), 1477–1481.
- 551 Dole, R. M., Spackman, J. R., Newman, M., Compo, G. P., Smith, C. A., Hartten,
552 L. M., . . . others (2018). Advancing science and services during the 2015/16 el
553 niño: The noaa el niño rapid response field campaign. *Bulletin of the American*
554 *Meteorological Society*, *99*(5), 975–1001.
- 555 Gazol, A., & Tíscar, P. (2020). Drought legacies are short, prevail in dry conifer
556 forests and depend on growth variability. *Journal of Ecology*, *108*(6), 2473-
557 2484.
- 558 Gudmundsson, L., Do, H. X., Leonard, M., & Westra, S. (2018). The global stream-
559 flow indices and metadata archive (gsim)–part 2: Quality control, time-series
560 indices and homogeneity assessment. *Earth System Science Data*, *10*(2),
561 787–804.
- 562 Harger, J. (1995). Enso variations and drought occurrence in indonesia and the
563 philippines. *Atmospheric Environment*, *29*(16), 1943–1955.
- 564 Haurwitz, M. W., & Brier, G. W. (1981). A critique of the superposed epoch anal-
565 ysis method: its application to solar–weather relations. *Monthly Weather Re-*
566 *view*, *109*(10), 2074–2079.
- 567 Higley, M. C., & Conroy, J. L. (2019). The hydrological response of surface water
568 to recent climate variability: A remote sensing case study from the central
569 tropical pacific. *Hydrological Processes*, *33*(16), 2227–2239.
- 570 Huang, B., Thorne, P. W., Banzon, V. F., Boyer, T., Chepurin, G., Lawrimore,
571 J. H., . . . Zhang, H.-M. (2017). Extended reconstructed sea surface tempera-
572 ture, version 5 (ersstv5): upgrades, validations, and intercomparisons. *Journal*
573 *of Climate*, *30*(20), 8179–8205.
- 574 Ibarra, D. E., David, C. P. C., & Tolentino, P. L. M. (2021). Evaluation and bias
575 correction of an observation-based global runoff dataset using streamflow ob-
576 servations from small tropical catchments in the philippines. *Hydrology and*
577 *Earth System Sciences*, *25*(5), 2805–2820.
- 578 Jorge-Romero, G., Celentano, E., Lercari, D., Ortega, L., Licandro, J. A., & Defeo,
579 O. (2021). Long-term and multilevel impact assessment of the 2015–2016
580 el niño on a sandy beach of the southwestern atlantic. *Science of The Total*
581 *Environment*, *775*, 145689.

- 582 Jose, A. M., & Cruz, N. A. (1999). Climate change impacts and responses in the
 583 philippines: water resources. *Climate research*, *12*(2-3), 77–84.
- 584 Kolusu, S. R., Shamsudduha, M., Todd, M. C., Taylor, R. G., Seddon, D., Kashaig-
 585 ili, J. J., . . . MacLeod, D. A. (2019). The el nino event of 2015–2016: cli-
 586 mate anomalies and their impact on groundwater resources in east and south-
 587 ern africa. *Hydrology and Earth System Sciences*, *23*(3), 1751–1762. doi:
 588 10.5194/hess-23-1751-2019
- 589 Kovats, R. S. (2000). El niño and human health. *Bulletin of the World Health Or-
 590 ganization*, *78*, 1127–1135.
- 591 Krishnamurthy, V., & Goswami, B. N. (2000). Indian monsoon–enso relationship on
 592 interdecadal timescale. *Journal of climate*, *13*(3), 579–595.
- 593 Kubota, H., Shirooka, R., Matsumoto, J., Cayan, E. O., & Hilario, F. D. (2017).
 594 Tropical cyclone influence on the long-term variability of philippine summer
 595 monsoon onset. *Progress in earth and planetary science*, *4*(1), 1–12.
- 596 Lansigan, F., De Los Santos, W., & Coladilla, J. (2000). Agronomic impacts of cli-
 597 mate variability on rice production in the philippines. *Agriculture, ecosystems
 598 & environment*, *82*(1-3), 129–137.
- 599 Lawrimore, J. H., Menne, M. J., Gleason, B. E., Williams, C. N., Wuertz, D. B.,
 600 Vose, R. S., & Rennie, J. (2011). An overview of the global historical clima-
 601 tology network monthly mean temperature data set, version 3. *Journal of
 602 Geophysical Research: Atmospheres*, *116*(D19).
- 603 Li, W., Fu, R., & Dickinson, R. E. (2006). Rainfall and its seasonality over the
 604 amazon in the 21st century as assessed by the coupled models for the ipcc ar4.
 605 *Journal of Geophysical Research: Atmospheres*, *111*(D2).
- 606 Lyon, B. (2004). The strength of el niño and the spatial extent of tropical drought.
 607 *Geophysical Research Letters*, *31*(21).
- 608 Lyon, B., Cristi, H., Verceles, E. R., Hilario, F. D., & Abastillas, R. (2006). Seasonal
 609 reversal of the enso rainfall signal in the philippines. *Geophysical research let-
 610 ters*, *33*(24).
- 611 Makanas, A. (1990). Pagasa [philippine atmospheric, geophysical and astronom-
 612 ical services administration] organization and climatic data resource in the
 613 philippines. *PCARRD Book Series (Philippines)*.
- 614 McPhaden, M. J. (2003). Tropical pacific ocean heat content variations and enso
 615 persistence barriers. *Geophysical research letters*, *30*(9).
- 616 Mendoza, B., Jauregui, E., Diaz-Sandoval, R., & Garci. (n.d.). Historical droughts in
 617 central mexico and their relation with el nino.
- 618 Nicholls, N. (1991). The el nino/southern oscillation and australian vegetation. *Veg-
 619 etatio*, *91*(1), 23–36.
- 620 Perez-Blanco, C. D., & Sapino, F. (2022). Economic sustainability of irrigation-
 621 dependent ecosystem services under growing water scarcity. insights from the
 622 reno river in italy. *Water Resources Research*, *58*, 2805–2820.
- 623 Perry, S., McGregor, S., Sen Gupta, A., England, M., & Maher, N. (2020). Pro-
 624 jected late 21st century changes to the regional impacts of the el niño-southern
 625 oscillation. *Climate Dynamics*, *54*(1), 395–412.
- 626 Poveda, G., Alvarez, D. M., & Rueda, O. A. (2011, June). Hydro-climatic
 627 variability over the Andes of Colombia associated with ENSO: a review
 628 of climatic processes and their impact on one of the Earth’s most impor-
 629 tant biodiversity hotspots. *Climate Dynamics*, *36*(11-12), 2233-2249. doi:
 630 10.1007/s00382-010-0931-y
- 631 Poveda, G., Jaramillo, A., Gil, M. M., Quiceno, N., & Mantilla, R. I. (2001). Season-
 632 ally in enso-related precipitation, river discharges, soil moisture, and vegetation
 633 index in colombia. *Water resources research*, *37*(8), 2169–2178.
- 634 Rao, M. P., Cook, E. R., Cook, B. I., Anchukaitis, K. J., D’Arrigo, R. D., Krusic,
 635 P. J., & LeGrande, A. N. (2019). A double bootstrap approach to super-
 636 posed epoch analysis to evaluate response uncertainty. *Dendrochronologia*, *55*,

- 637 119–124. doi: 10.1016/j.dendro.2019.05.001
- 638 Rao, M. P., Cook, E. R., Cook, B. I., D’Arrigo, R. D., Palmer, J. G., Lall, U., . . .
639 others (2020). Seven centuries of reconstructed brahmaputra river discharge
640 demonstrate underestimated high discharge and flood hazard frequency. *Nature*
641 *communications*, *11*(1), 1–10.
- 642 Rimbu, N., Dima, M., Lohmann, G., & Stefan, S. (2004). Impacts of the north
643 atlantic oscillation and the el niño–southern oscillation on danube river flow
644 variability. *Geophysical Research Letters*, *31*(23).
- 645 Santoso, A., Mcphaden, M. J., & Cai, W. (2017). The defining characteristics of
646 enso extremes and the strong 2015/2016 el niño. *Reviews of Geophysics*, *55*(4),
647 1079–1129. doi: <https://doi.org/10.1002/2017RG000560>
- 648 Schmidt, N., Lipp, E., Rose, J., & Luther, M. E. (2001). Enso influences on seasonal
649 rainfall and river discharge in florida. *Journal of Climate*, *14*(4), 615–628.
- 650 Sheffield, J., & Wood, E. F. (2007). Characteristics of global and regional drought,
651 1950–2000: Analysis of soil moisture data from off-line simulation of the ter-
652 restrial hydrologic cycle. *Journal of Geophysical Research: Atmospheres*,
653 *112*(D17). doi: <https://doi.org/10.1029/2006JD008288>
- 654 Simpson, H., Cane, M., Herczeg, A., Zebiak, S., & Simpson, J. (1993). Annual
655 river discharge in southeastern australia related to el nino-southern oscillation
656 forecasts of sea surface temperatures. *Water Resources Research*, *29*(11),
657 3671–3680.
- 658 Stoelzle, M., Stahl, K., Morhard, A., & Weiler, M. (2014). Streamflow sensitivity to
659 drought scenarios in catchments with different geology. *Geophysical Research*
660 *Letters*, *41*(17), 6174–6183. doi: <https://doi.org/10.1002/2014GL061344>
- 661 Stuecker, M. F., Tigchelaar, M., & Kantar, M. B. (2018, 08). Climate variability im-
662 pacts on rice production in the philippines. *PLOS ONE*, *13*(8), 1–17. doi: 10
663 .1371/journal.pone.0201426
- 664 Tolentino, P. L. M., Poortinga, A., Kanamaru, H., Keesstra, S., Maroulis, J., David,
665 C. P. C., & Ritsema, C. J. (2016). Projected impact of climate change on
666 hydrological regimes in the philippines. *PLoS One*, *11*(10), e0163941.
- 667 Trenberth, K. E. (1997). The definition of el nino. *Bulletin of the American Meteo-*
668 *rological Society*, *78*(12), 2771–2778.
- 669 Turkington, T., Timbal, B., & Rahmat, R. (2019). The impact of global warming on
670 sea surface temperature based el niño–southern oscillation monitoring indices.
671 *International Journal of Climatology*, *39*(2), 1092–1103.
- 672 Van Oldenborgh, G. J., Hendon, H., Stockdale, T., L’Heureux, M., De Perez, E. C.,
673 Singh, R., & Van Aalst, M. (2021). Defining el niño indices in a warming
674 climate. *Environmental Research Letters*, *16*(4), 044003.
- 675 Van Rossum, G., & Drake, F. L. (2009). *Python 3 reference manual*. Scotts Valley,
676 CA: CreateSpace.
- 677 Venkatappa, M., Sasaki, N., Han, P., & Abe, I. (2021). Impacts of droughts and
678 floods on croplands and crop production in southeast asia – an application of
679 google earth engine. *Science of The Total Environment*, *795*, 148829. doi:
680 <https://doi.org/10.1016/j.scitotenv.2021.148829>
- 681 Villafuerte, M. Q., Matsumoto, J., & Kubota, H. (2015). Changes in extreme rainfall
682 in the philippines (1911–2010) linked to global mean temperature and enso. *In-*
683 *ternational Journal of Climatology*, *35*(8), 2033–2044.
- 684 Villafuerte II, M. Q., Matsumoto, J., Akasaka, I., Takahashi, H. G., Kubota, H., &
685 Cinco, T. A. (2014). Long-term trends and variability of rainfall extremes in
686 the philippines. *Atmospheric Research*, *137*, 1–13.
- 687 Wang, B., Luo, X., Yang, Y.-M., Sun, W., Cane, M. A., Cai, W., . . . Liu, J. (2019).
688 Historical change of el niño properties sheds light on future changes of extreme
689 el niño. *Proceedings of the National Academy of Sciences*, *116*(45), 22512–
690 22517.
- 691 Williams, A. D., & Gochoco, J. C. (1924). *Surface water supply of the philippine is-*

692 *lands volume iii.*

- 693 Yang, Y., McVicar, T. R., Donohue, R. J., Zhang, Y., Roderick, M. L., Chiew,
694 F. H., . . . Zhang, J. (2017). Lags in hydrologic recovery following an extreme
695 drought: Assessing the roles of climate and catchment characteristics. *Water*
696 *Resources Research*, 53(6), 4821–4837.
- 697 Yatagai, A., Kamiguchi, K., Arakawa, O., Hamada, A., Yasutomi, N., & Kitoh,
698 A. (2012). Aphrodite: Constructing a long-term daily gridded precipitation
699 dataset for asia based on a dense network of rain gauges. *Bulletin of the Amer-*
700 *ican Meteorological Society*, 93(9), 1401 - 1415. Retrieved from [https://](https://journals.ametsoc.org/view/journals/bams/93/9/bams-d-11-00122.1.xml)
701 journals.ametsoc.org/view/journals/bams/93/9/bams-d-11-00122.1.xml
702 doi: 10.1175/BAMS-D-11-00122.1
- 703 Zhu, C., Cavazos, T., & Lettenmaier, D. P. (2007). Role of antecedent land surface
704 conditions in warm season precipitation over northwestern mexico. *Journal of*
705 *Climate*, 20(9), 1774–1791.

1 **Supporting Information for ”A decrease in river**
2 **discharge and rainfall amount, from a 100-year**
3 **data-set, in response to El Niño events on the**
4 **interannual temporal scale for the Philippines”**

Natasha Sekhon^{1,2}, Carlos Primo C. David³, Mart Cyrel M. Geronia³,

Manuel Justin G. Custado³, Daniel E. Ibarra^{1,2}

5 ¹Department of Earth, Environmental and Planetary Science, Brown University, Providence, Rhode Island 02912, USA

6 ²Institute at Brown for Environment and Society, Brown University, Providence, Rhode Island 02912, USA

7 ³National Institute of Geological Sciences, University of the Philippines, Diliman, Quezon City, 1101, Philippines

8 **Introduction** The following figures highlight the data processing steps for river discharge
9 and rainfall amount data. The supplemental table includes the list of river discharge and
10 rainfall amount sites, the time covered by the measurements, and the original source of
11 the data used.

Corresponding author: N. Sekhon, Department of Earth, Environmental and Planetary Science
and Institute at Brown for Environment and Society, Brown University, Providence, Rhode Island
02912, USA. (natasha_sekhon@brown.edu)

February 14, 2022, 7:47pm

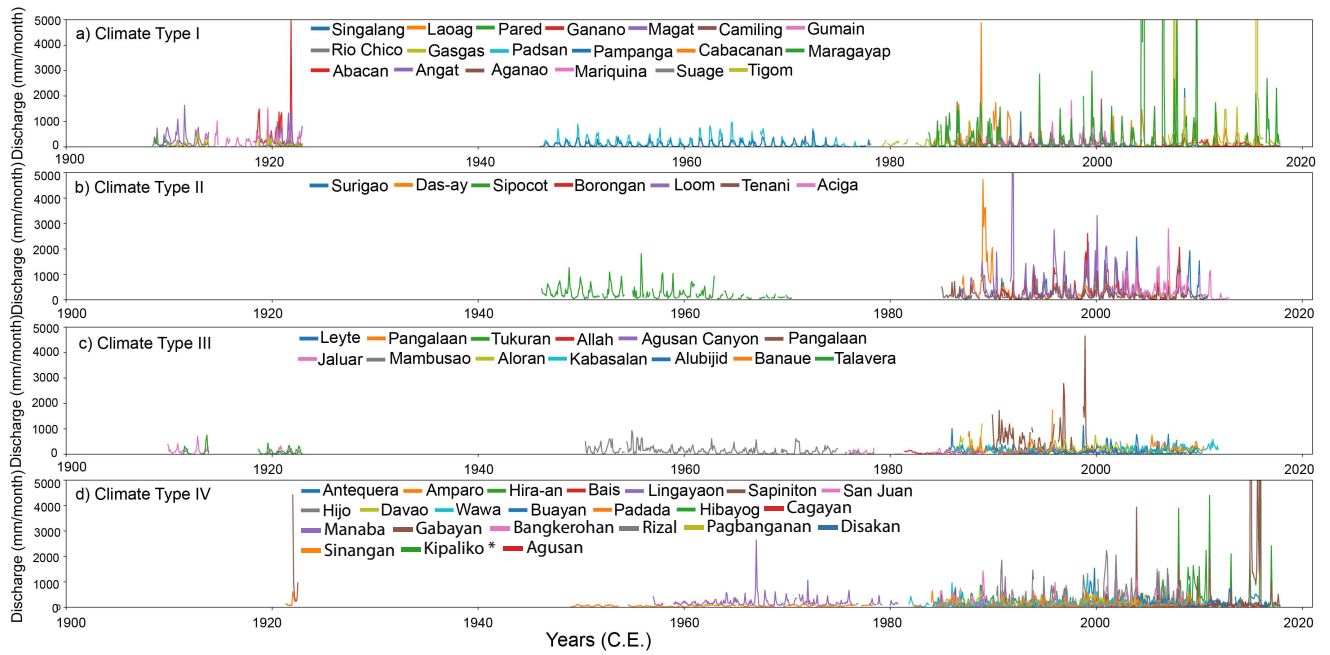


Figure S1. Time series of 61 discharge station data used in this study. River discharge station data that fall under Climate Type I (a), II (b), III (c), IV (d). *Kipaliko has been updated since Ibarra et al. (2021).

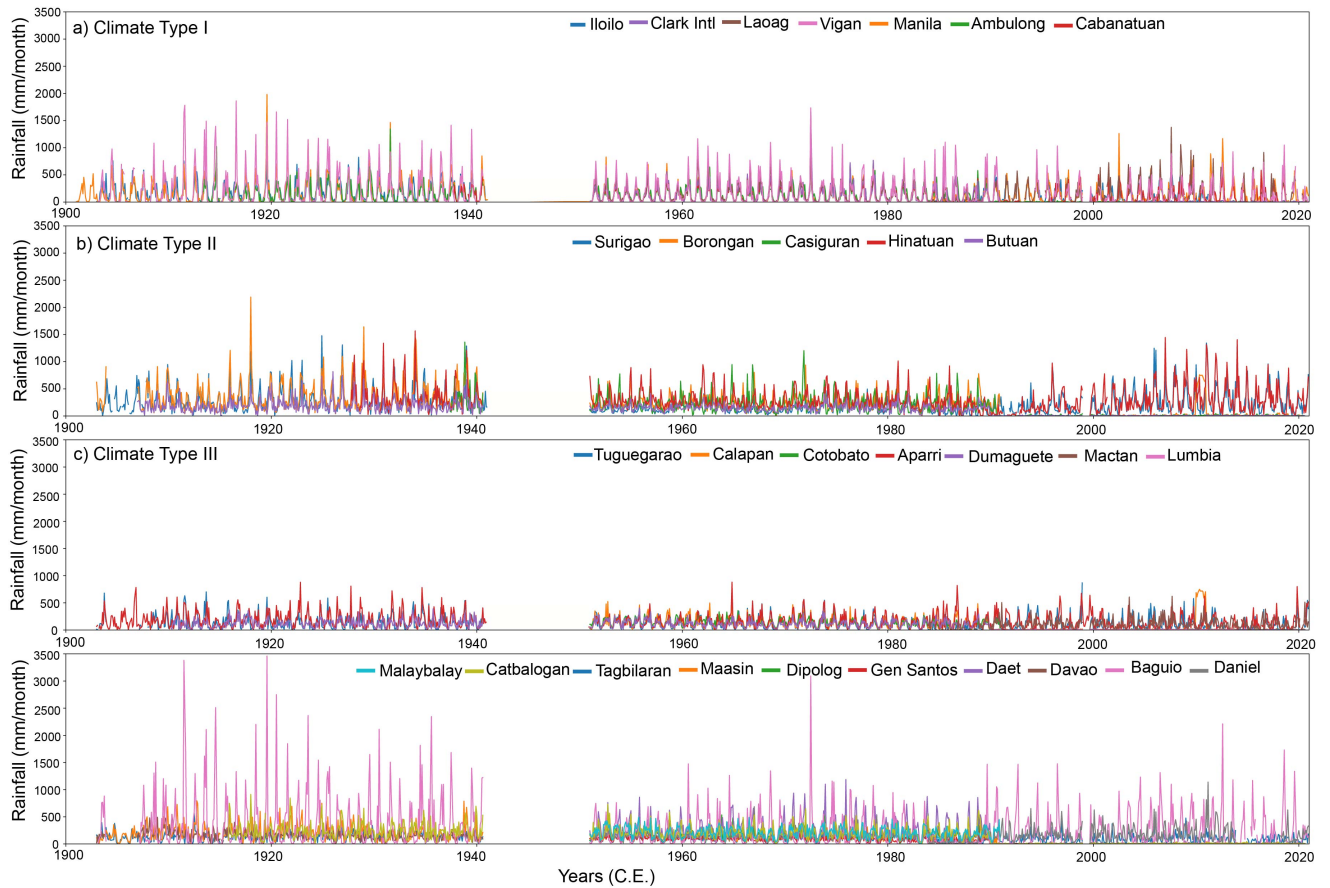


Figure S2. Time series of 29 rainfall data used in this study. Rainfall station and gridded data that fall under Climate Type I (a), II (b), III (c), IV (d).

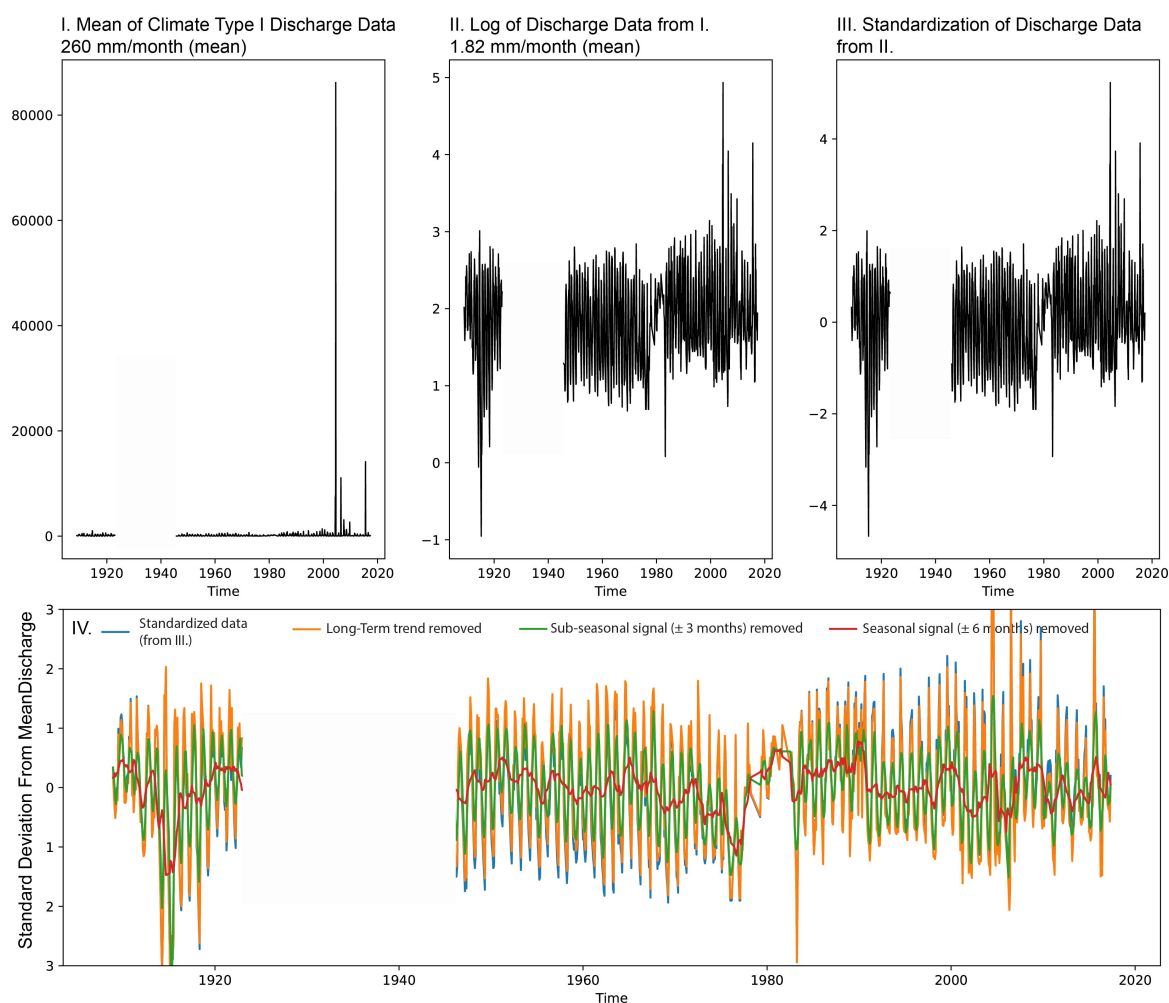


Figure S3. Data reduction steps for river discharge data that fall under Climate Type I

I. Mean of area normalized discharge data in mm/month. II. Log of the mean area normalized discharge data. III. Standardized (interchangeable with scaled) discharge data around the log mean. This data is used to remove the long term trends (Supp. Figure. 4). IV. Standardized data plotted with data where long-term trends were removed using a polynomial fit. The sub-seasonal (± 3) and seasonal (± 6) signal removed data is also plotted.

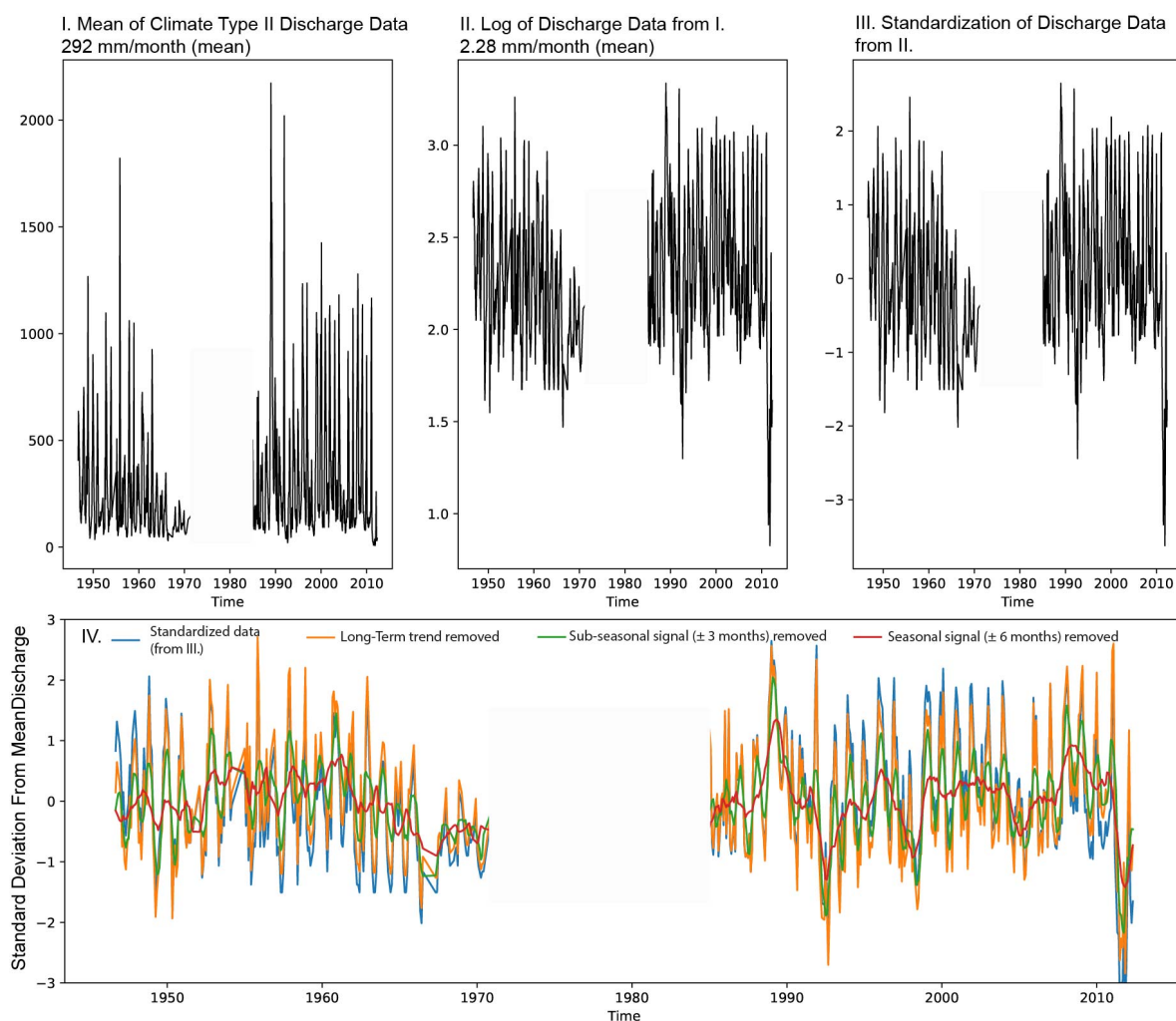


Figure S4. Data reduction steps for river discharge data that fall under Climate Type II

I. Mean of area normalized discharge data in mm/month. II. Log of the mean area normalized discharge data. III. Standardized (interchangeable with scaled) discharge data around the log mean. This data is used to remove the long term trends (Supp. Figure. 4). IV. Standardized data plotted with data where long-term trends were removed using a polynomial fit. The sub-seasonal (± 3) and seasonal (± 6) signal removed data is also plotted.

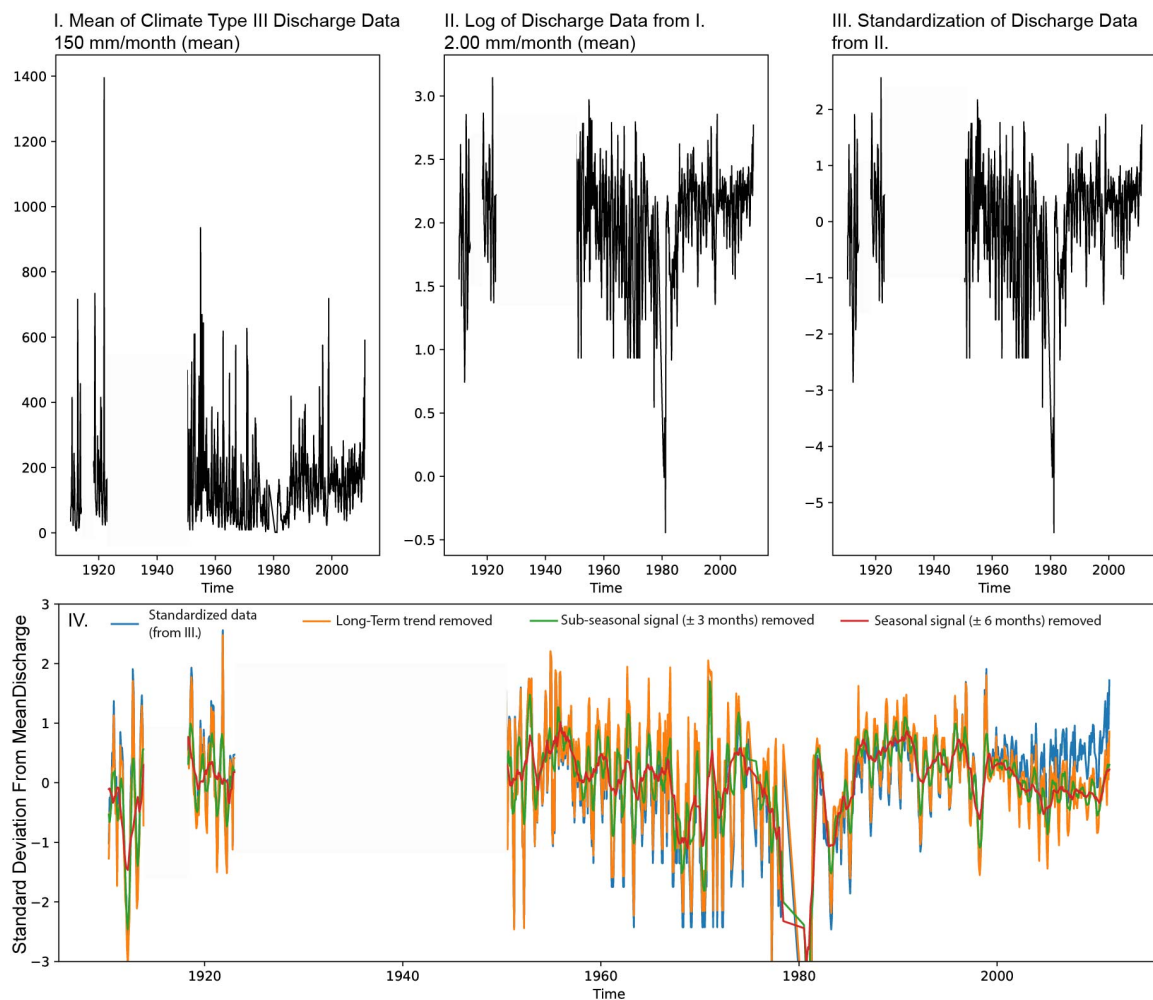


Figure S5. Data reduction steps for river discharge data that fall under Climate Type III

I. Mean of area normalized discharge data in mm/month. II. Log of the mean area normalized discharge data. III. Standardized discharge data around the log mean. This data is used to remove the long term trends (Supp. Figure. 4). IV. Standardized data plotted with data where long-term trends were removed using a polynomial fit. The sub-seasonal (± 3) and seasonal (± 6) signal removed data is also plotted.

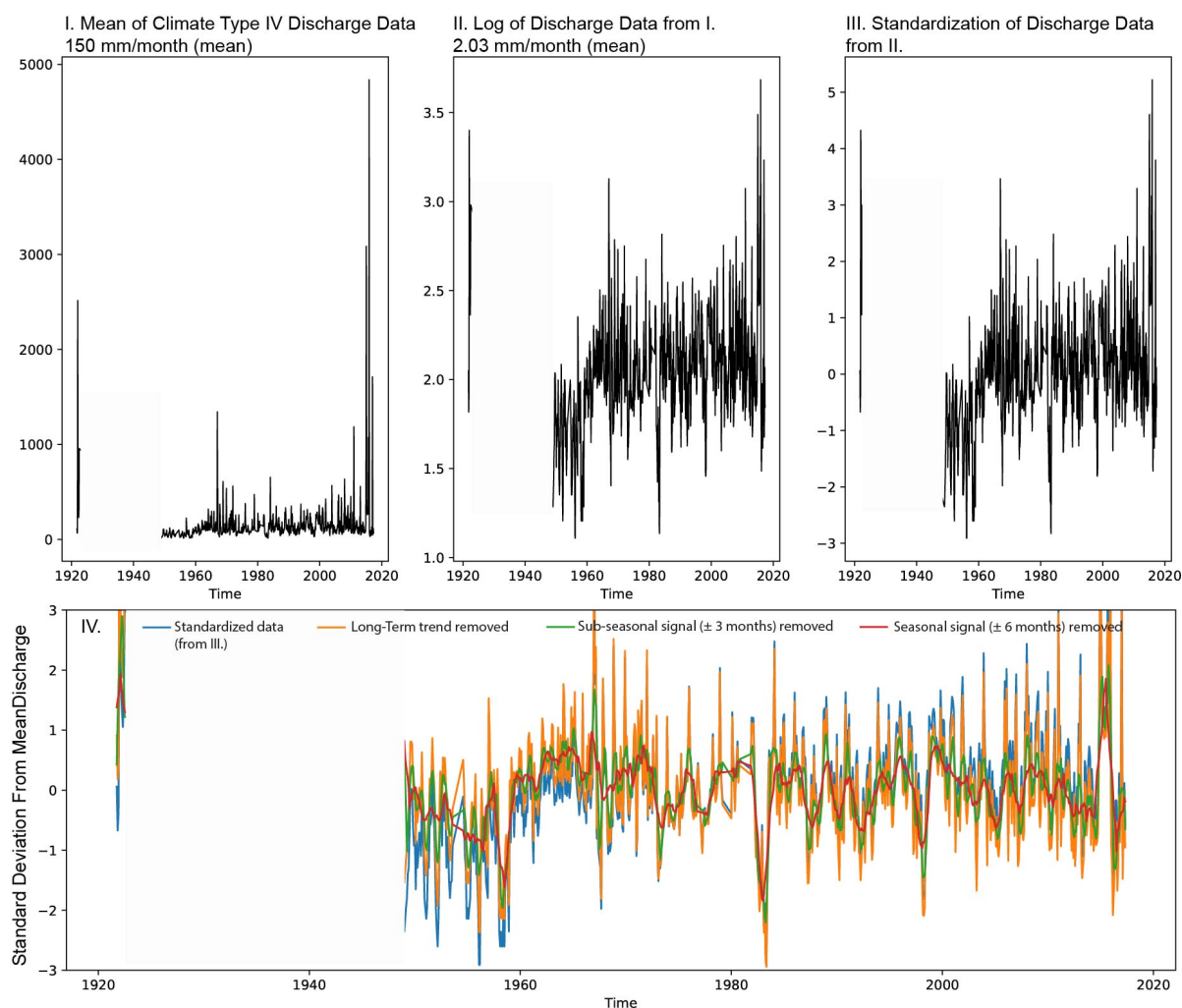


Figure S6. Data reduction steps for river discharge data that fall under Climate Type IV

I. Mean of area normalized discharge data in mm/month. II. Log of the mean area normalized discharge data. III. Standardized discharge data around the log mean. This data is used to remove the long term trends (Supp. Figure. 4). IV. Standardized data plotted with data where long-term trends were removed using a polynomial fit. The sub-seasonal (± 3) and seasonal (± 6) signal removed data is also plotted.

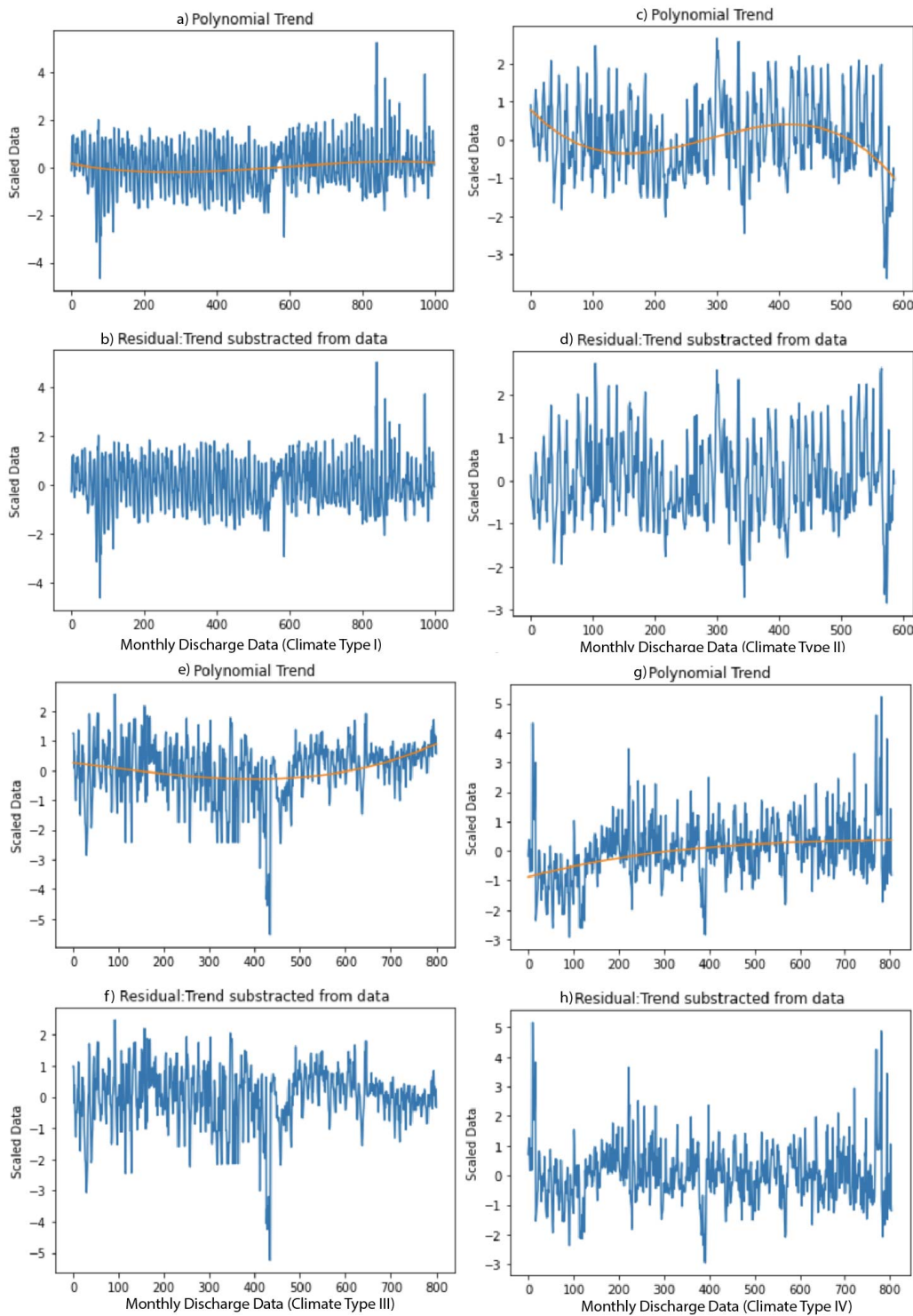


Figure S7. Subtracting long-term trends from standardized monthly discharge data for Climate Type I (a-b), II (c-d), III (e-f), IV (g-h). The orange line (in a,c,e,g) indicates the long-term trend using a polynomial fit (order =3). The residual discharge data (in b,d,f,h) is used for the remaining analyses.

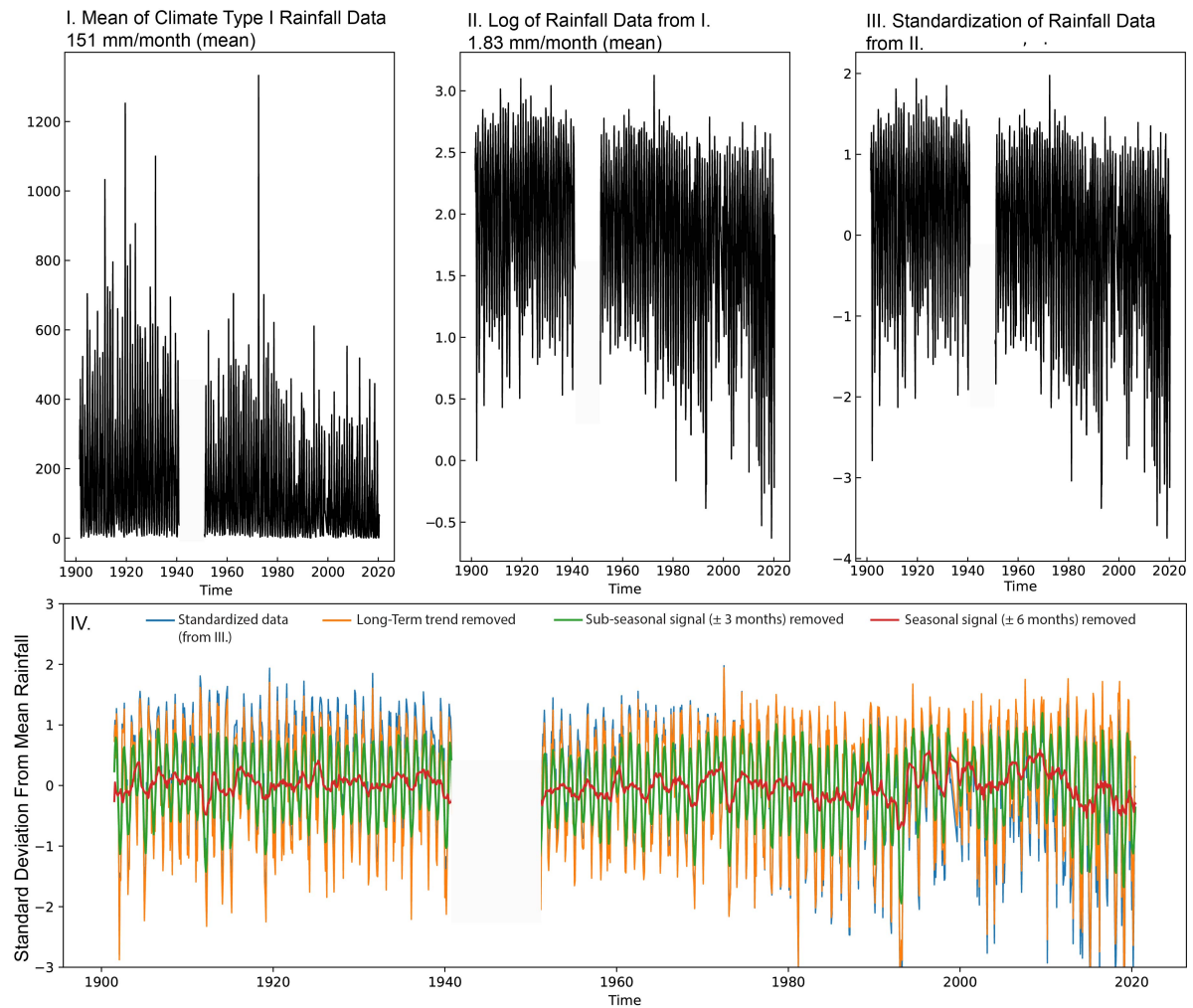


Figure S8. Data reduction steps for rainfall amount data that fall under Climate Type I. I. Mean of rainfall amount data in mm/month. II. Log of the mean rainfall data. III. Standardized rainfall data around the log mean. This data is used to remove the long term trends (Supp. Figure. 6). IV. Standardized data plotted with data where long-term trends were removed using a polynomial fit. The sub-seasonal (± 3) and seasonal (± 6) signal removed data is also plotted.

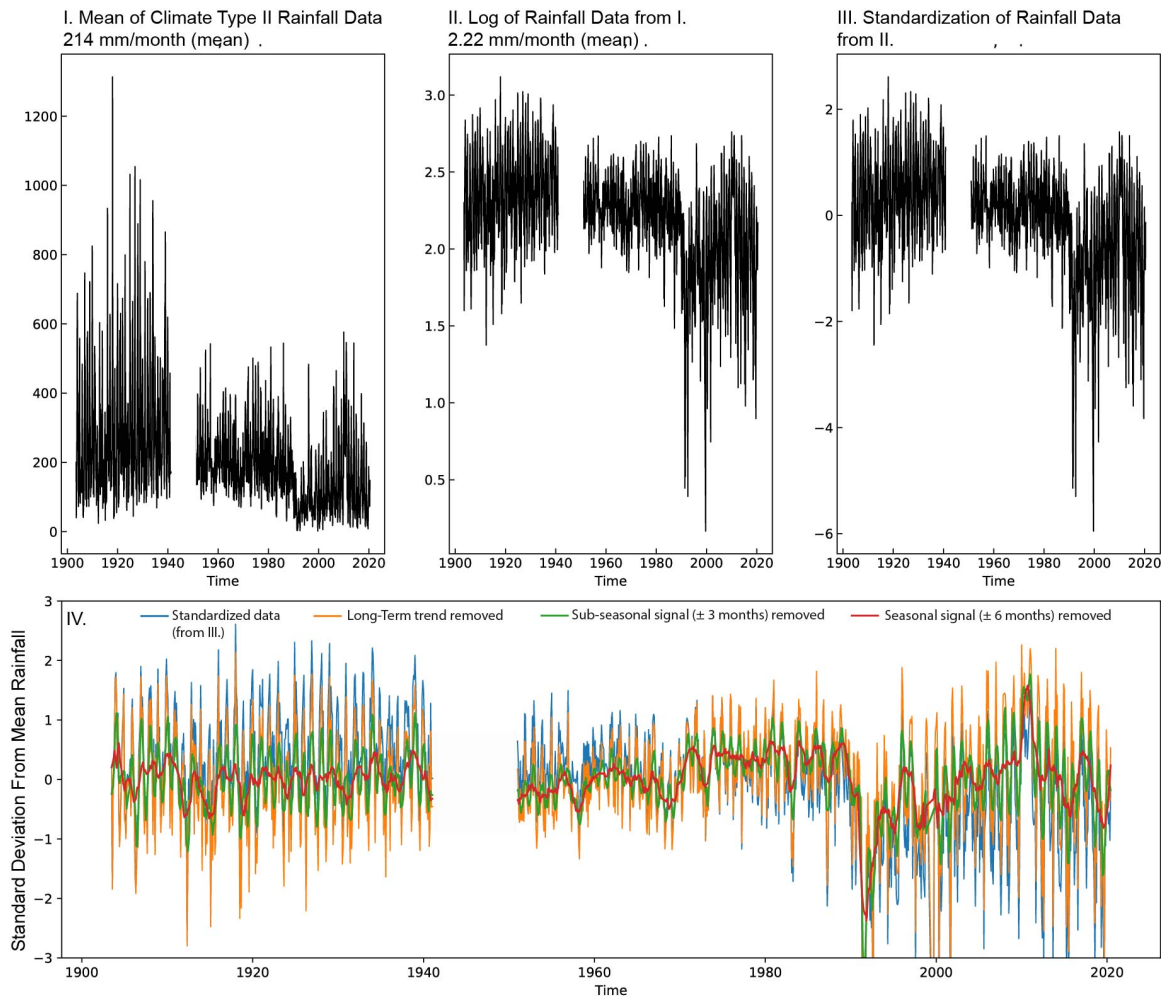


Figure S9. Data reduction steps for rainfall amount data that fall under Climate Type II
 I. Mean of rainfall amount data in mm/month. II. Log of the mean rainfall data. III. Standardized rainfall data around the log mean. This data is used to remove the long term trends (Supp. Figure. 6). IV. Standardized data plotted with data where long-term trends were removed using a polynomial fit. The sub-seasonal (± 3) and seasonal (± 6) signal removed data is also plotted.

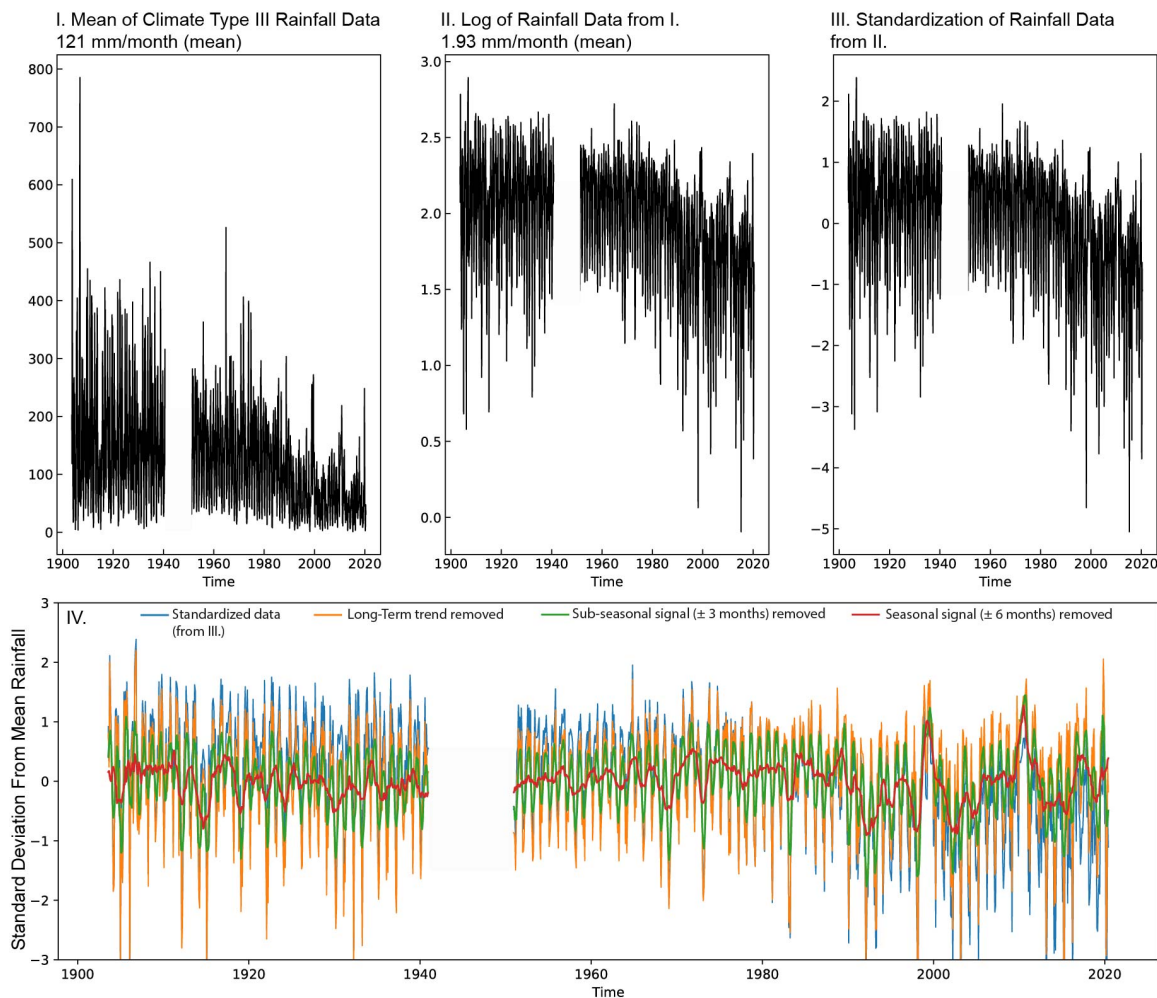


Figure S10. Data reduction steps for rainfall amount data that fall under Climate Type III. I. Mean of rainfall amount data in mm/month. II. Log of the mean rainfall data. III. Standardized rainfall data around the log mean. This data is used to remove the long term trends (Supp. Figure. 6). IV. Standardized data plotted with data where long-term trends were removed using a polynomial fit. The sub-seasonal (± 3) and seasonal (± 6) signal removed data is also plotted.

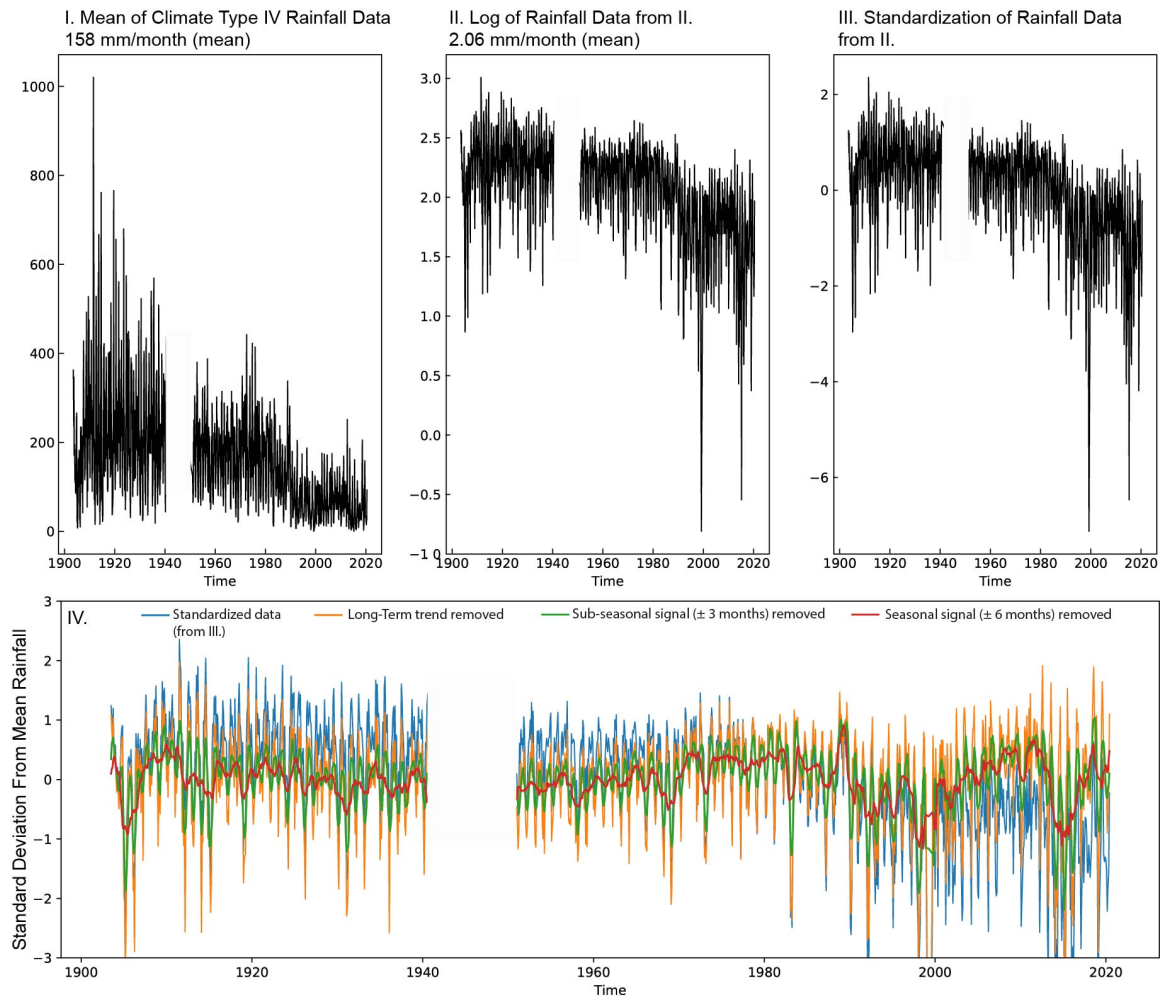


Figure S11. Data reduction steps for rainfall amount data that fall under Climate Type IV I. Mean of rainfall amount data in mm/month. II. Log of the mean rainfall data. III. Standardized rainfall data around the log mean. This data is used to remove the long term trends (Supp. Figure. 6). IV. Standardized data plotted with data where long-term trends were removed using a polynomial fit. The sub-seasonal (± 3) and seasonal (± 6) signal removed data is also plotted.

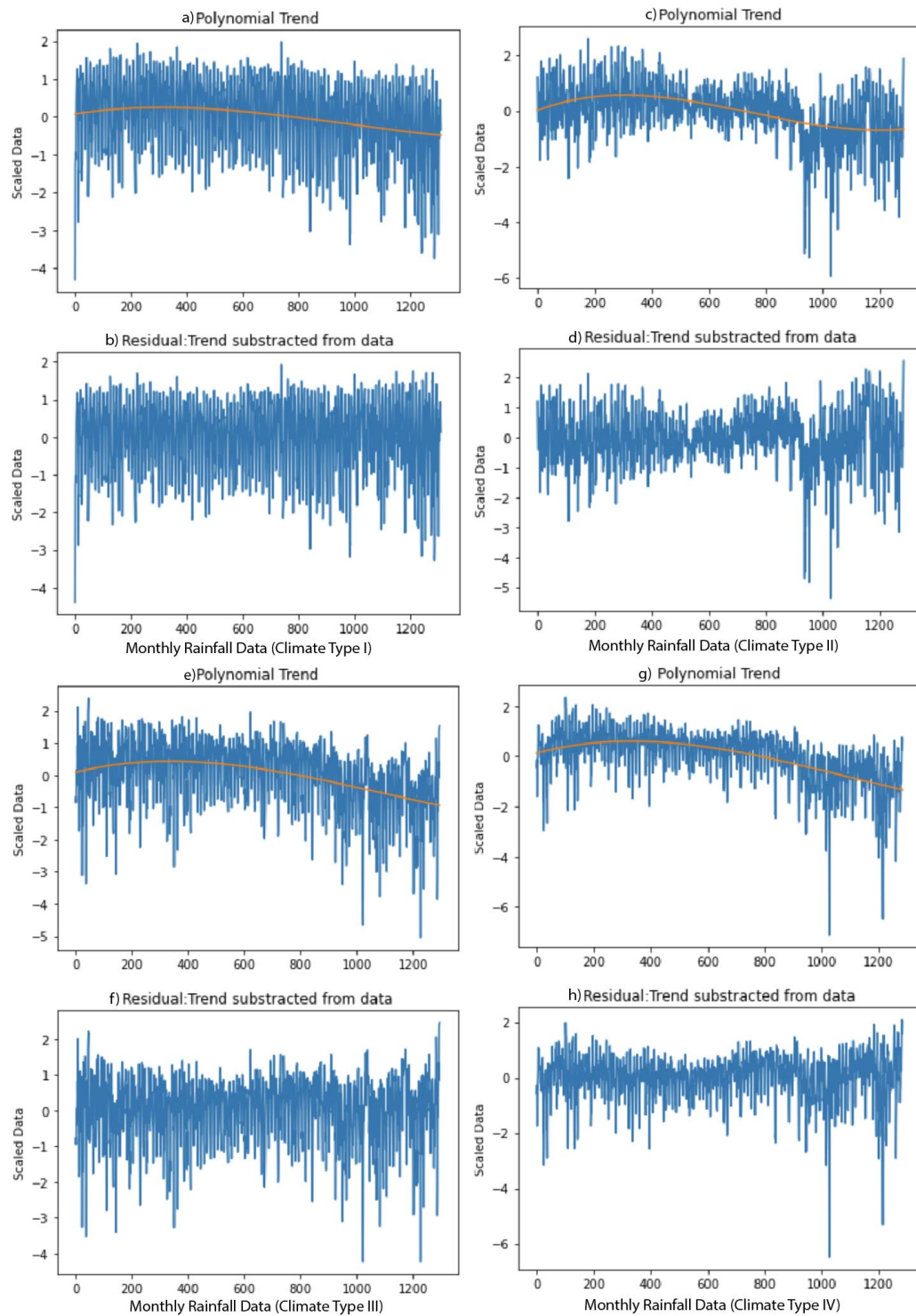


Figure S12. Subtracting long-term trends from scaled monthly rainfall data for Climate Type I (a-b), II (c-d), III (e-f), IV (g-h). The orange line (in a,c,e,g) indicates the long-term trend using a polynomial fit (order =3). The residual rainfall data (in b,d,f,h) is used for the remaining analyses.

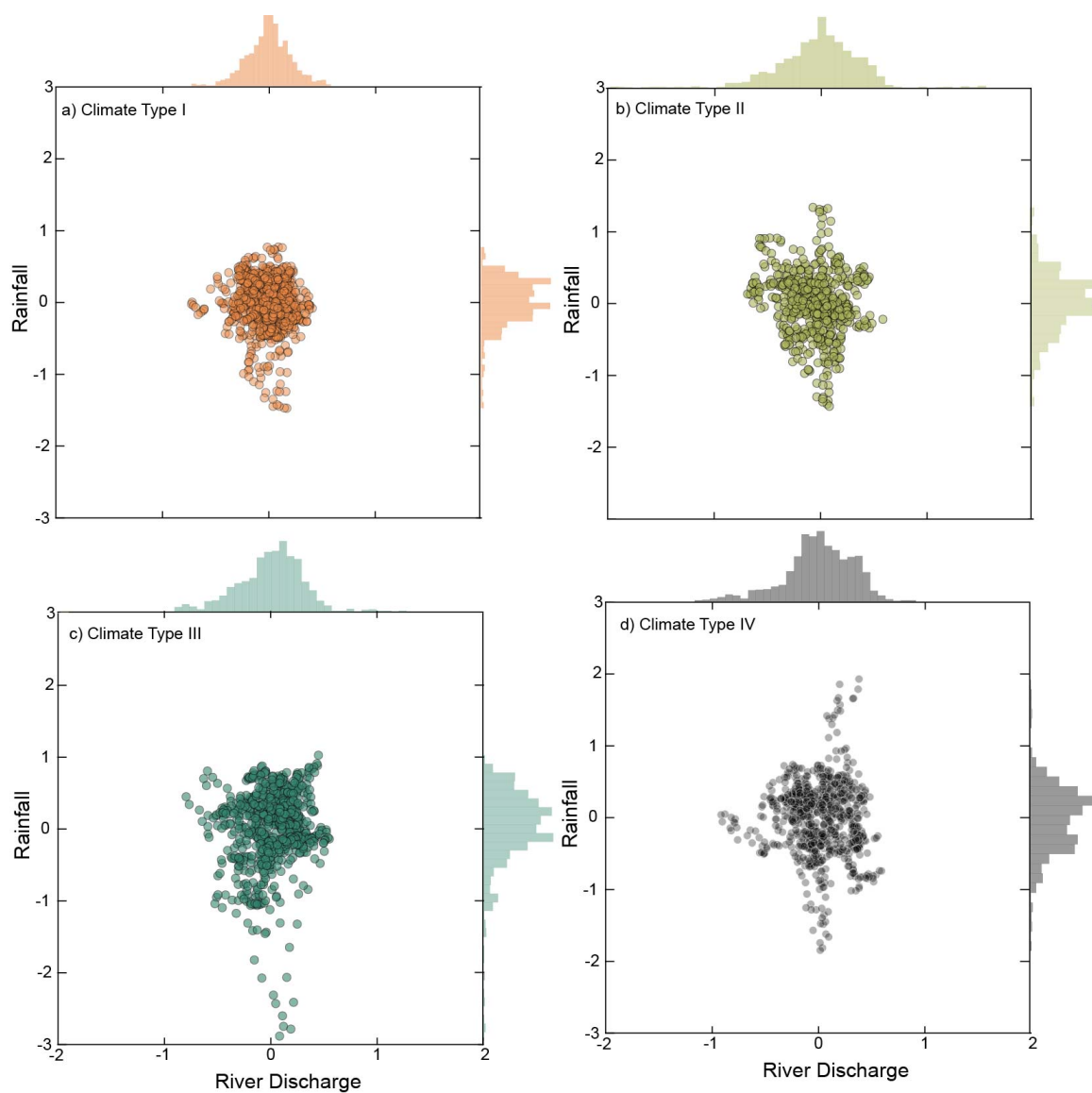


Figure S13. Bivariate plot of rainfall amount and river discharge data based on Climate Types.

Table S1. River discharge station name with Latitude and Longitude, Time Period Covered, Climate Type, and data source. Data from Ibarra et al. (2021); Williams and Gochoco (1924)

River Name	Latitude	Longitude	Years Covered	Climate Type	Dataset
Singalang River	17.56	120.64	1984-2015	1	used in Ibarra et al. (2021)
Antequera River	9.76	123.9	1984-2016	4	used in Ibarra et al. (2021)
Amparo River	10.10	124.91	1985-2007	4	used in Ibarra et al. (2021)
Hira-an River	11.26	124.67	1986-2010	4	used in Ibarra et al. (2021)
Leyte River	11.28	124.56	1985-2007	3	used in Ibarra et al. (2021)
Surigao River	9.73	125.50	1986-2010	2	used in Ibarra et al. (2021)
Bais River	9.88	124.14	1989-2015	4	used in Ibarra et al. (2021)
Lingayaon River	11.19	124.86	1957-1991	4	used in Ibarra et al. (2021)
Sapiniton River	11.32	124.82	1984-2010	4	used in Ibarra et al. (2021)
Laoag River	18.20	120.58	1921-1922;1984-2016	1	used in Ibarra et al. (2021) + BPW
Pared River	17.90	121.68	1983-1996	1	used in Ibarra et al. (2021)
Ganano River	16.69	121.55	1918-1921;1986-2001	1	used in Ibarra et al. (2021) + BPW
Magat River	16.58	121.25	1920-1922;1986-2002	1	used in Ibarra et al. (2021) + BPW
Camiling River	15.61	120.37	1985-2017	1	used in Ibarra et al. (2021)
Gumain River	14.91	120.56	1985-2001	1	used in Ibarra et al. (2021)
Rio Chico River	15.44	120.75	1985-2006	1	used in Ibarra et al. (2021)
San Juan River	14.21	121.15	1986-1999	4	used in Ibarra et al. (2021)
Pangalaan River	13.30	121.19	1989-1999	3	used in Ibarra et al. (2021)
Das-ay River	10.37	125.16	1987-2007	2	used in Ibarra et al. (2021)
Tukuran River	7.87	123.59	1986-2009	3	used in Ibarra et al. (2021)
Hijo River	7.39	125.83	1986-2016	4	used in Ibarra et al. (2021)
Cagayan River	8.39	124.61	1991-2004	4	used in Ibarra et al. (2021)
Davao River	7.09	125.59	1984-1999	4	used in Ibarra et al. (2021)
Allah River	6.67	124.56	1980-1994	3	used in Ibarra et al. (2021)
Agusan Canyon River	8.32	124.80	1986-2004	3	used in Ibarra et al. (2021)
Wawa River	8.81	125.70	1981-2010	4	used in Ibarra et al. (2021)
Buayan River	6.31	125.26	1986-2004	4	used in Ibarra et al. (2021)
Gasgas River	18.08	120.83	1978-1988	1	used in Ibarra et al. (2021)
Jalaur River	10.93	122.67	1909-13;1918-22;1976-88	3	used in Ibarra et al. (2021) + BPW
Padsan River	18.08	120.7	1946-1979	1	used in Ibarra et al. (2021)
Pampanga River	15.17	120.78	1946-1977	1	used in Ibarra et al. (2021)
Sipocot River	13.81	122.99	1946-1970	2	used in Ibarra et al. (2021)
Mambusao River	11.26	122.57	1919-1922;1950-1978	3	used in Ibarra et al. (2021) + BPW
Padada River	6.66	125.28	1949-1978	4	used in Ibarra et al. (2021)
Aloran River	8.42	123.82	1978-2003	3	used in Ibarra et al. (2021)
Cabacanan River	18.58	120.8	1979-2017	1	used in Ibarra et al. (2021)
Maragayap River	16.75	120.37	1908-09;1912;1919-22; 2004-17	1	used in Ibarra et al. (2021) + BPW
Abacan River	15.11	120.70	2004-2017	1	used in Ibarra et al. (2021)
Hibayog River	9.87	124.14	2004-2017	4	used in Ibarra et al. (2021)
Manaba River	9.63	124.13	2001-2016	4	used in Ibarra et al. (2021)
Gabayon River	9.84	124.45	1922; 2001-2017	4	used in Ibarra et al. (2021) + BPW
Bangkerohan River	10.34	124.83	1984-1990;2000-2009	4	used in Ibarra et al. (2021)
Borongon River	11.62	125.40	1990-2008	2	used in Ibarra et al. (2021)
Loom River	11.38	125.23	1986-2004	2	used in Ibarra et al. (2021)
Pagbanganan River	10.63	124.86	1984-2008	4	used in Ibarra et al. (2021)
Rizal River	11.38	124.90	1990-2008	4	used in Ibarra et al. (2021)
Tenani River	11.80	125.12	1985-2001	2	used in Ibarra et al. (2021)
Disakan River	8.48	123.04	1985-1991;1997-2000	4	used in Ibarra et al. (2021)
Kabasalan River	7.83	122.77	2002-2011	3	used in Ibarra et al. (2021)
Sindangan River	8.21	123.05	1990-2003	4	used in Ibarra et al. (2021)
Alubijid River	8.57	124.47	1991-2009	3	used in Ibarra et al. (2021)
Kipaliko River	7.60	125.68	2004-2016	4	used in Ibarra et al. (2021)
Banaue River	16.91	121.06	1987-1995;2005-2010	3	used in Ibarra et al. (2021)
Aciga River	9.26	125.57	2002-2015	2	used in Ibarra et al. (2021)
Agusan River	7.99	126.03	1921-22;1982;1984-87; 1989-2010	4	used in Ibarra et al. (2021) + BPW
Angat River	14.90	120.79	1909-1913;1918-1922	1	BPW
Suague River	10.94	122.51	1908-1913;1918-1922	1	BPW
Tigom River	10.76	122.54	1909-1913;1918-1922	1	BPW
Mariquina River	14.61	121.07	1912-1922	1	BPW
Aganao River	10.78	122.51	1910-1913;1918-1922	1	BPW
Talavera River	15.35	120.55	1911-1913;1918-1922	3	BPW

Table S2. Rainfall station name with with Latitude and Longitude, Time Period Covered, Climate Type, and data source. Data from Yatagai et al. (2012); Kubota et al. (2017); Lawrimore et al. (2011)

Rainfall Station	Latitude	Longitude	Years Covered	Climate Type	Dataset
Vigan	17.55	120.35	1903-40;1951-90; 1991-2020	1	PWB; APHRODITE; Modern
Tagbilaran	9.66	123.85	1903-40;1951-90;1991-2020	4	PWB; APHRODITE; Modern
Maasin City	10.13	124.86	1903-40;1951-90;1991-2020	4	PWB; APHRODITE; Modern
Surigao	9.78	125.48	1903-40;1951-90;1991-2020	2	PWB; APHRODITE; Modern
Laoag City	18.18	120.53	1951-90; 1991-2020	1	APHRODITE; Modern
Tuguegarao	17.63	121.75	1903-40;1951-90; 1991-2020	3	PWB; APHRODITE;Modern
Clark Intl	15.18	120.55	1951-90;1991-2020	1	APHRODITE; Modern
Cabanatuan	15.46	120.95	1951-90;1991-2018	1	APHRODITE; Modern
Ambulong	14.08	121.05	1903-40;1951-90;1991-2020	1	PWB; APHRODITE; Modern
Calapan	13.41	121.18	1951-90;1991-2020	3	APHRODITE; Modern
Cotobato	7.16	124.21	1951-90;1992-2020	3	APHRODITE; Modern
Dipolog	8.6	123.35	1951-90;1991-2020	4	APHRODITE; Modern
Gen Santos	6.11	125.18	1951-90;1991-2020	4	APHRODITE; Modern
Mactan	10.31	123.98	1951-90;1991-2020	3	APHRODITE; Modern
Daet	14.13	122.98	1951-90;1991-2020	4	APHRODITE; Modern
Lumbia	8.41	124.61	1991-2018	3	Modern
Davao	7.13	125.65	1903-40;1991-2020	4	PWB; Modern
Aparri	18.36	121.63	1903-40;1951-90;1991-2020	3	PWB; APHRODITE;Modern
Baguio City	16.4	120.6	1903-40;1951-90;1991-2020	4	PWB; APHRODITE; Modern
Borongan	11.66	125.45	1903-40;1951-90;2001-2020	2	PWB; APHRODITE; Modern
Daniel Romualdez	11.22	125.02	1951-90;1991-2020	4	APHRODITE; Modern
Iloilo	10.7	122.56	1903-40;1991-2011	1	PWB; Modern
Catbalogan	11.78	124.88	1903-40;1951-90;1991-2020	4	PWB; APHRODITE; Modern
Malaybalay	8.15	125.13	1951-90	4	APHRODITE
Casiguran	16.26	122.13	1951-90;1991-2020	2	APHRODITE; Modern
Hinatuan	8.36	126.33	1927-40;1951-90;1991-2020	2	PWB;APHRODITE; Modern
Manila	14.58	120.98	1903-40;1951-90;1991-2020	1	PWB; APHRODITE; Modern
Dumaguete	9.33	123.3	1903-40;1951-90;1991-2020	3	PWB; APHRODITE; Modern
Butuan	8.95	125.48	1901-40;1951-90;1991-2020	2	PWB; APHRODITE; Modern

References

- 12 Ibarra, D. E., David, C. P. C., & Tolentino, P. L. M. (2021). Evaluation and bias correc-
13 tion of an observation-based global runoff dataset using streamflow observations from
14 small tropical catchments in the philippines. *Hydrology and Earth System Sciences*,
15 *25*(5), 2805–2820.
- 16 Kubota, H., Shiroyaka, R., Matsumoto, J., Cayanan, E. O., & Hilario, F. D. (2017).
17 Tropical cyclone influence on the long-term variability of philippine summer monsoon
18 onset. *Progress in earth and planetary science*, *4*(1), 1–12.
- 19 Lawrimore, J. H., Menne, M. J., Gleason, B. E., Williams, C. N., Wuertz, D. B., Vose,
20 R. S., & Rennie, J. (2011). An overview of the global historical climatology network
21 monthly mean temperature data set, version 3. *Journal of Geophysical Research:*
22 *Atmospheres*, *116*(D19).
- 23 Williams, A. D., & Gochoco, J. C. (1924). *Surface water supply of the philippine islands*
24 *volume iii*.
- 25 Yatagai, A., Kamiguchi, K., Arakawa, O., Hamada, A., Yasutomi, N., & Kitoh, A.
26 (2012). Aphrodite: Constructing a long-term daily gridded precipitation dataset for
27 asia based on a dense network of rain gauges. *Bulletin of the American Meteorological*
28 *Society*, *93*(9), 1401 - 1415. Retrieved from [https://journals.ametsoc.org/view/](https://journals.ametsoc.org/view/journals/bams/93/9/bams-d-11-00122.1.xml)
29 journals/bams/93/9/bams-d-11-00122.1.xml doi: 10.1175/BAMS-D-11-00122
30 .1
-